

PCBSchemaGen: Constraint-Guided Schematic Design via LLM for Printed Circuit Boards (PCB)

Huanghaohe Zou¹ Peng Han¹ Emad Nazerian¹ Alex Q. Huang¹

Abstract

Printed Circuit Board (PCB) schematic design plays an essential role in all areas of electronic industries. Unlike prior works that focus on digital or analog circuits alone, PCB design must handle heterogeneous digital, analog, and power signals while adhering to real-world IC packages and pin constraints. Automated PCB schematic design remains unexplored due to the scarcity of open-source data and the absence of simulation-based verification. We introduce **PCBSchemaGen**, the first training-free framework for PCB schematic design that comprises LLM agent and Constraint-guided synthesis. Our approach makes three contributions: **1.** an LLM-based code generation paradigm with iterative feedback with domain-specific prompts. **2.** a verification framework leveraging a real-world IC datasheet derived Knowledge Graph (KG) and Subgraph Isomorphism encoding pin-role semantics and topological constraints. **3.** an extensive experiment on 23 PCB schematic tasks spanning digital, analog, and power domains. Results demonstrate that PCBSchemaGen significantly improves design accuracy and computational efficiency. All source code, KG and benchmark open sourced at: <https://github.com/HZou9/PCBSchemaGen>.

1. Introduction

Over the past decades, Printed Circuit Boards (PCBs) have been the essence of the modern electronics industry, enabling the integration of complex integrated circuit (IC) technology into large-scale systems. The wide range of PCB applications, from consumer electronics to aerospace, medical devices, robotics, electric vehicles, renewable en-

ergy system and generative AI hardware infrastructure (Kim et al., 2011; Pecht, 2009; Huang et al., 2011; Amano et al., 2018), has driven the demand for rapid and reliable PCB design methodologies. The market size of PCB reached to USD 74.12 billion in 2025, with a projected goal to USD 113.5 billion by 2032 (Fortune Business Insights, 2026). However, the traditional PCB schematic design workflow is heavily dependent on manual effort, often requiring months or even years of iteration to validate a usable design. This expertise is highly diverse, necessitating extensive experience to master the intricacies of various ICs and their complex interconnections. Furthermore, PCBs must simultaneously integrate high-speed digital logic routing, precision analog circuitry, and high-current power delivery networks, making this field significantly more challenging than traditional digital logic or analog-only IC circuit design.

PCB schematic design is the critical interlink between IC-level design and board-level layout, which remains unexplored and still predominantly a manual process, it fundamentally faces three major challenges. First, unlike digital circuit design that benefits from abundant open-source code and benchmarks (Liu et al., 2023b; Chen et al., 2021), PCB schematic designs are scarce for large scale training. Second, PCB schematic design lacks verification tool. Many references used SPICE simulation for analog circuit simulation (Lai et al., 2025; Bhandari et al., 2024), SPICE is designed for idealized functional simulation, not for validating PCB schematic correctness under real IC package and pin-level constraints. therefore, it is neither sufficient nor appropriate as a primary verifier for the task studied in this paper. Existing work only focuses on suggestion (Liu et al., 2024a) or transformation from existing netlists (Matsuo et al., 2024) rather than generative design tasks. Third, while traditional analog and digital circuit tasks utilize ideal components(e.g. ideal MOS or R), PCB schematic design tasks are interacting with real IC components with different packages and pin constraints, which prevents the direct application of generation from fixed datasets or fine-tuned LLMs, which lack the flexibility to adapt to different real-world IC chips.

To face the aforementioned challenges, we propose **PCB-SchemaGen**, the first training-free code generation frame-

¹Semiconductor Power Electronics Center(SPEC), University of Texas at Austin, Austin, TX, USA. Correspondence to: Alex Q. Huang <aqhhuang@utexas.edu>.

work for PCB schematic with constrained code synthesis and verification. Since PCB schematics can be translated as SKiDL Python style code (Vandenbout, 2025), our key approach is to leverage LLM to be proposal SKiDL generator for code generation. We built a datasheet-driven knowledge graph (KG) and Subgraph Isomorphism (SI) based verifier to ensure the generated schematic correctness. This decoupled architecture not only avoids reliance on large-scale training data, but also ensures the interpretability, reliability and reproducibility of verification through rules. Our contributions are summarized as follows:

- **Training-free code generation paradigm:** We employ an LLM as a proposal generator for SKiDL code. With domain-specific prompting, Chain-of-Thought (CoT) and In-context Learning (ICL) (Dong et al., 2023a), it can directly synthesize executable design code without fine-tuning. An iterative feedback workflow leverages interpretable messages from the verifier for higher code-synthesis success rate.
- **KG & SI driven multi-phase verifier:** We construct a domain knowledge graph from open source real-world IC datasheets with pin-role semantic, multiple constraint types and topological constraints. A KG and SI based driven verification framework provides specific feedback and interpretable error messages.
- **PCB schematic tasks Benchmarking:** To our knowledge, we curated a first benchmark for evaluate the PCB generative ability of LLMs. This benchmark comprises 23 unique circuits that span digital, analog, and power domains, in which each task is associated with real-world IC components. We demonstrated PCB-SchemaGen provided end-to-end capability from natural language specification to KiCAD PCB layout file ready for following task, with real world IC packages. This benchmark validates its reproducibility and practicality, which can serve as a comprehensive evaluation platform for future research.

2. Preliminaries and Related Work

2.1. Traditional PCB Schematic Design Workflow

PCB circuit design involves multiple key stages: function definition, component selection, schematic design generation with multiple iterations, PCB component placement, PCB routing and prototyping. The general PCB tasks with multiple subproblems (e.g. netlist/placement/layout) is NP-hard due to its equivalence to multiple choices of IC components, multi-terminal routing and constrained optimization problems. Based on the intended PCB functions, human experts are required to select the correct IC chips and values, define the interconnections, and generate the schematic

design. Some recent works have been shown to automate PCB component placement and routing. LayoutCopilot (Liu et al., 2024a) proposed a Multi-LLM agents interactive layout framework. FanoutNet (Li et al., 2023) realized PCB fanout routability. For circuit topology generation, Autocircuit-RL (Vijayaraghavan et al., 2025b) proposed a RL driven LLM method to explore circuit topologies. However, none of these prior works have addressed the PCB schematic design automated generation problem. Unlike sole digital or circuit design, which benefits from standardized languages (e.g. Verilog and SPICE) (Thomas & Moorby, 2002) and mature simulation tools, PCB schematic capture is vendor specific, this makes large scale training difficult. Since IC component selection and schematic design require human intelligence, domain knowledge, and meticulous attention to detail, this topic is never explored thoroughly.

2.2. Existing Circuit Design

Existing circuit design works mainly focus on digital or analog circuits solely. Generative AI shows great potential in Verilog circuit generation. Early work Chip-Chat (Blocklove et al., 2023) proposed the possibility of Human-AI collaboration, but it lacks the ability to directly generate Verilog code. ChipNeMo (Liu et al., 2023a) outperforms GPT-4 on chip design tasks through domain adaptation. Both VeriGen (Thakur et al., 2024) and Deep-RTL (Liu et al., 2025) enhanced code quality via fine-tuning and unified representation learning. However, PCB schematic data scarcity prevents similar approaches from fine-tuning LLMs. BetterV (Pei et al., 2024) introduced discriminative guidance to achieve controlled generation, and the QiMeng series (Zhang et al., 2025b;c; Zhu et al., 2025) only focus on Verilog digital circuit synthesis. AutoChip (Thakur et al., 2023) proved the efficacy of iterative feedback mechanisms in improving generation success rates, while GPT4AIGChip (Fu et al., 2023) showcased the potential of In-Context Learning (ICL). However, these works primarily focus on internal digital logic design and lack modeling of board-level packaging and pin constraints.

For analog circuit generation, AnalogCoder (Lai et al., 2025) modeled analog circuits as PySpice code and used prompt engineering for training-free generation, but it lacks the flexibility to handle complex multi-component connections. AnalogGenie series (Gao et al., 2025; Gao et al.) employed graph generative methods to discover novel circuit topologies. Artisan (Chen et al., 2024) introduced knowledge-driven natural language descriptions for op-amp circuit generation. However, due to its narrow focus, it highly depends on netlist tuples generated by human experts. LaMAGIC2 (Chang et al., 2025) modeled the problem as LLM-supervised generation, which still relies on large-scale topology datasets. AmpAgent (Liu et al., 2024b) proposed multi-agent pipelines, which still exhibit dependency on human

experience. CktGNN (Dong et al., 2023b) employed Graph Neural Networks for analog circuit synthesis. ADO-LLM (Yin et al., 2024) combines LLM and Bayesian Optimization (BO) for faster convergence, but LLMs didn't understand the circuit fundamentally. Reinforcement Learning (RL) is also introduced for optimizing IC layout (Mirhoseini et al., 2021; Lai et al., 2023). Ref(Vijayaraghavan et al., 2025a) combines LLM and RL for generation, but only within ideal analog circuit scale. TopoSizing (Wei et al., 2025) created a framework for Bayesian optimization-based LLM understanding, but the approach is not generative. PE-GPT (Lin et al., 2025) focuses on power electronics circuit design by leveraging Retrieval-Augmented Generation (RAG) to access domain knowledge. However, it cannot generate complete circuits, and the RAG mechanism is prone to hallucinations regarding specific pin rules and constraints.

Compared with IC-level digital or analog circuit design, board-level PCB related generative AI works are still scarce. LayoutCopilot (Liu et al., 2024a) proposed interactive LLM agents for PCB layout, but it doesn't cover schematic design. Ref(Wang et al., 2025) only explored LLM's ability to understand chip package, but still not end-to-end generative. PCBRouting (Zhang et al., 2025a) only focused on LLM routing task, but lacks schematic generation still. Existing generative methods mainly employ a one-pass strategy, which lacks closed-loop verification (Chen et al., 2023). Though Self-Debug and MetaGPT (Olausson et al., 2023; Hong et al., 2023) demonstrated the potential of self-repair and multi-agent collaboration, injecting IC-level physical constraints (e.g., electrical specifications from IC datasheets) into LLM reasoning remains challenging. AMSNet-KG (Shi et al., 2025) shows the potential by constructing Knowledge Graphs (KG) but only anchored by fixed dataset. CircuitLM (Hasan et al., 2026) uses multi-LLMs for circuit generation and verification, but LLM based verification is prone to hallucinations and lacks deterministic, rule-based guarantees. A score based verification system is proposed, but it cannot represent the specific circuit violation that can feedback to LLMs. EESchematic (Liu & Chitnis, 2025) uses vision-LLM, but limited to small-scale circuits with idealized components. MathVista (Lu et al., 2024) also proves that VLLM may introduce visual hallucination and lacks precision and reproducibility for precise PCB design. WiseEDA (Jin et al., 2025) only focuses on passive component parameters optimization, not end-to-end code circuit generation. CROP (Pan et al., 2025) employs Retrieval-Augmented Generation(RAG) over embedded Verilog circuits, but still not synthesizing from natural language. Ref (Yan et al., 2022) only focuses on component-level PCB planning, not generative schematic synthesis. Ref (Kumar Jha et al., 2024) introduces feedback mechanisms for Verilog generation, but limited to syntax and functional correctness. Ref (Plettenberg et al., 2025) only explores simple

tasks with four IC pins by GNN, and it lacks feedback mechanism. Overall, prior work mostly focuses on functional simulation, generation from datasets, or syntax-level correction, whereas PCB schematic generation under real IC package and pin constraints remains largely unaddressed. In this work, **PCBSchemaGen** constructs an IC-domain datasheet-driven KG that anchors LLM generation in real-world physical IC constraints.

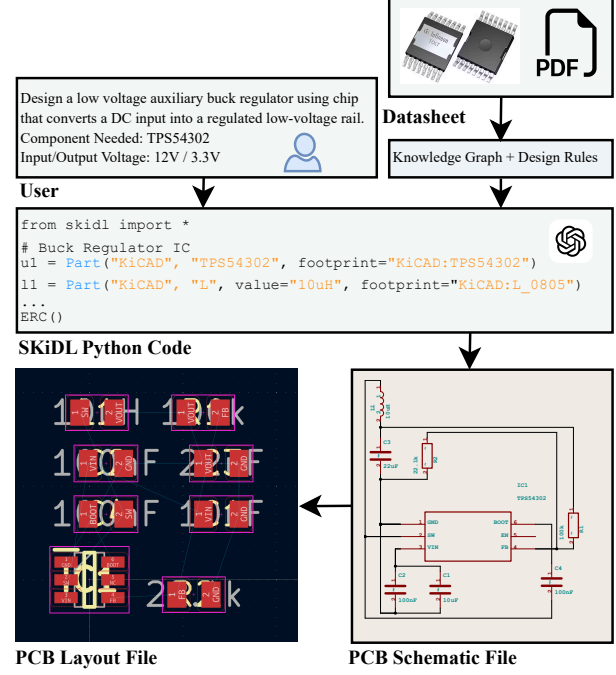


Figure 1. Overview of the PCBSchemaGen framework workflow. (a) User inputs natural language description of PCB schematic design task, it can be digital, analog or power task, or mix of them. (b) PCBSchemaGen agent read the KG and designed rules from IC datasheets. (c) The agent generates SKiDL code. (d) Correct SKiDL code generates KiCAD PCB schematic file. (e) KiCAD generates PCB Layout file that is ready for routing.

3. Approach

PCBSchemaGen is an LLM-based framework for translating natural language PCB schematic design specification to LLM to generate SKiDL code (Vandenbout, 2025; Wang et al., 2023; Qin et al., 2023), as shown in Fig. 1. We proposed a sophisticated prompt design methodology to enhance the LLM's comprehension proficiency, circuit connectivity awareness, and learning adaptability. To improve generation accuracy, we proposed a multi-stage verification framework based on IC datasheet driven Knowledge Graph (KG), electrical design rules, and Subgraph Isomorphism (SI) checking for topology verification. For PCB schematics involving real IC packages and pin-level constraints, no scalable functional or electrical performance verifier currently exists, making datasheet-grounded structural verification a

necessary and practical abstraction. The multi-stage verification feedback provides the failure information to the LLM for iterative refinement. The basic circuit library also enables the reuse of validated sub-circuits for complex tasks, which mimics the human expert design experience.

3.1. Prompt Design

A well designed prompt is critical for LLM to understand the task, the domain knowledge and the electrical connection logic. A good KiCAD PCB layout file can be imported from many languages, including Python based SKiDL language, netlist format and JSON format (Pei et al., 2024; Li et al., 2024; Wu et al., 2024). However, We select SKiDL as the target representation because Python-based hardware description languages offer the highest information density. Furthermore, since the vast majority of state-of-the-art LLMs have undergone extensive fine-tuning on Python code bases, SKiDL serves as the most effective medium for translating functional requirements into executable schematics (DeLorenzo et al., 2024). Furthermore, SKiDL’s Python foundation allows LLMs to understand the package information and the pin constraints effectively.

We also add more technique in prompt design. We integrated in-context learning (ICL) (Dong et al., 2023a) by providing multiple examples of PCB schematic design tasks with different grammars. By offering an example of isolated voltage amplifier circuit, we provide details of SKiDL code structure, component instantiation, and net connections, which enhance the one-shot learning capability. Chain-of-Thought (CoT) (Wei et al., 2023) is also introduced to guide the LLM to reason about the circuit connectivity and semantic learning step by step. This prompt engineering approaches substantially improves the LLM’s ability to understand complex circuit topologies and pin-role semantics. Comprehensive prompts are provided in Appendix.

3.2. Knowledge Graph (KG) Design

Since LLMs lack the physical understanding of IC components, their pin-role semantics, and special physical constraints due to physical packages, we construct a domain-specific Knowledge Graph (KG) from real-world IC datasheets to guide the LLM generation and verification, while save the need for uploading large datasheets to LLMs context window. The KG captures the essential information of IC components, including pin roles, electrical properties, topological constraints, and isolation boundaries, etc.

We formally define the Knowledge Graph as a tuple $\mathcal{KG} = (\mathcal{C}, \mathcal{R}, \mathcal{A}, \Phi, \mathcal{I})$, where:

- \mathcal{C} is the set of component types.
- \mathcal{R} is the set of 36 pin role types.

- $\mathcal{A} : \mathcal{C} \rightarrow 2^{\text{Attributes}}$ is the attribute function mapping components to their physical properties.
- $\Phi : \mathcal{C} \rightarrow 2^{\text{Constraints}}$ is the constraint function defining electrical and topological rules.
- \mathcal{I} is the isolation boundary function.

Pin Roles & Constraints Set up: We define a semantic labeling function $\rho : \mathcal{P}_c \rightarrow \mathcal{R}$ for each component type $c \in \mathcal{C}$, mapping its pins to one of 36 roles. This abstraction enables role-based pattern matching across heterogeneous IC families, decoupling verification logic from vendor-specific pin naming conventions. Since each IC has unique datasheet for injecting physical constraints, injecting entire PDF datasheet to LLMs is infeasible due to the limited context window.

We built KG by encoding essential device rules and constraints in a structured form, reducing the token footprint per IC component from approximately **16k** tokens (typical datasheet length) to average **300** token, achieving a **30 to 70 times reduction** in context usage while preserving functional and electrical constraints. Detailed KG construction process is provided in Appendix below.

3.3. Verification Pipeline.

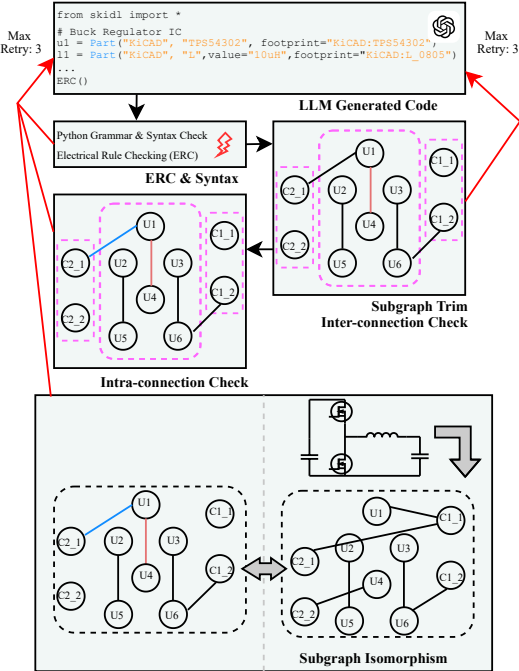


Figure 2. The multi-stage verification flow of PCBSchemaGen.

Since PCB schematic design failure can arise from multiple aspects, we propose a multi-stage verification framework, as shown in Fig. 2. We firstly give the Python and SKiDL syntax check to ensure the generated code is executable, followed by built in Electrical Rule Checking (ERC) to

Algorithm 1 Unified Topology Verification (Rules + Skeleton Semantics)

Require: σ_{gen} , \mathcal{R} , System Template \mathcal{T} , \mathcal{KG} , Passive Set \mathcal{P}
Ensure: (ok, \mathcal{E})

- 1: $\mathcal{E} \leftarrow \emptyset$
- 2: $G \leftarrow \text{BuildBipartiteGraph}(\sigma_{\text{gen}})$
- 3: $G_p \leftarrow \text{BuildTopologyGraph}(\sigma_{\text{gen}}, \mathcal{KG})$ {Reduced net-role graph}
- 4: **for** each $r = (\tau, ep_a, ep_b) \in \mathcal{R}$ **do**
- 5: $N_a, N_b \leftarrow \text{Resolve}(\{ep_a, ep_b\}, \sigma_{\text{gen}})$
- 6: **if** $N_a = \emptyset \vee N_b = \emptyset$ **then**
- 7: $\mathcal{E} \leftarrow \mathcal{E} \cup \{\text{ResErr}(r)\}$
- 8: **else if** $\neg \text{EvalRule}(\tau, N_a, N_b, G, \mathcal{P})$ **then**
- 9: $\mathcal{E} \leftarrow \mathcal{E} \cup \{\text{RuleViol}(r)\}$
- 10: **end if**
- 11: **end for**
- 12: $\Pi \leftarrow \text{Ports}(\mathcal{T}, \sigma_{\text{gen}})$
- 13: $\mathcal{H} \leftarrow \text{InferPrimitives}(G_p, \Pi)$
- 14: **for** each semantic constraint $c \in \mathcal{T.C}$ **do**
- 15: **if** $\neg \text{CheckConstraint}(c, G_p, \Pi, \mathcal{H}, \mathcal{P})$ **then**
- 16: $\mathcal{E} \leftarrow \mathcal{E} \cup \{\text{SemViol}(c)\}$
- 17: **end if**
- 18: **end for**
- 19: **return** $(\mathcal{E} = \emptyset, \mathcal{E})$

ensure all pins are properly connected and placed. Then we transformed circuit into bipartite graph for following verification.

A circuit topology is formally represented as a bipartite graph $G = (V_C \cup V_N, E)$, where components and nets constitute two disjoint sets of vertices. The edges within this graph represent the electrical connections between component pins and their corresponding nets. Formally:

$$G = (V_C \cup V_N, E) \quad (1)$$

where:

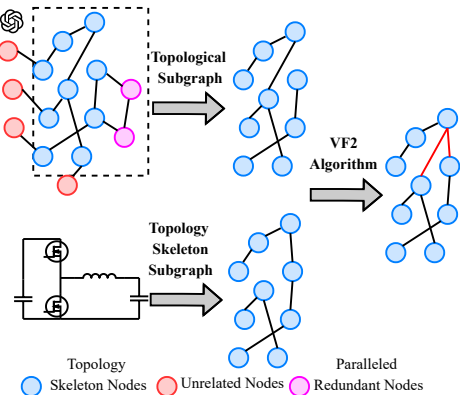


Figure 3. Illustration of the Subgraph Isomorphism (SI) based topological verification process.

- $V_C = \{c_1, c_2, \dots, c_m\}$ is the set of component vertices.
- $V_N = \{n_1, n_2, \dots, n_k\}$ is the set of net vertices.
- $E \subseteq V_C \times V_N$ is the edge set representing pin-to-net connections.

We firstly trim the subgraph that only contains critical components and nets, followed by inter-connection check. This step ensures all connection violations within the pins belongs to same component are detected(e.g. short-circuit between VCC and GND). Then, an intra-connection check between key components and other IC or passive components is performed to ensure all violations between components pins are detected. Both verification KG and design rules are employed for these checks. For composite circuits like power converters or mixed-signal systems, topology skeleton semantics extraction and understanding is critical for a successful generation, so we further perform Subgraph Isomorphism(SI) based topological verification to ensure the topology correctness and completeness. We further define a circuit isomorphism from a generated circuit G_{gen} to a reference circuit G_{ref} as a mapping $\phi : V(G_{\text{gen}}) \rightarrow V(G_{\text{ref}})$ such that:

$$\forall (u, v) \in E(G_{\text{gen}}) : (\phi(u), \phi(v)) \in E(G_{\text{ref}}) \quad (2)$$

Based on this formulation, the topology verification problem can be reduced to a subgraph isomorphism problem:

$$\text{Verify}(\sigma_{\text{gen}}, \sigma_{\text{ref}}, \mathcal{R}) \Leftrightarrow \exists \text{ injective } \phi : G_{\mathcal{R}} \hookrightarrow G_{\text{gen}} \quad (3)$$

where $G_{\mathcal{R}}$ is the rule graph encoding all topological constraints and design rules. We use VF2 algorithm (Cordella et al., 2004) for efficient subgraph isomorphism checking. The overall unified topology verification process is summarized in Algorithm 1 and illustrated in Fig. 3. More details of the verification pipeline and algorithm details, such as end-to-end error message that LLM can understand semantics and topologies, SI with various constraints tolerance, are provided in Appendix. Proposed multi-stage verification ensures real IC components correct functionality, including sensing network, Op-amp based amplifier and pass-filter design, digital logic interconnection, and power converter topologies. The correctness of the verification framework is validated through human expert evaluation in next section.

3.4. feedback Loop & Subcircuit Library

Since the multi-stage SI based verification can precisely locate the failure reason, including which nodes or edges violate which KG knowledge, which rules or where topology skeleton is violated, we can provide those specific feedback messages to LLM while suggesting which component pins

or nets are violated. This interpretable feedback not only enhances LLM to figure out the mistakes in complex networks, but also helps LLM to understand the task requirements better. We performed ablation study in next section to validate the effectiveness of feedback-refinement loop. We introduce three types of feedback messages:

- **Detailed and specific error messages:** Includes syntax, ERC errors, and subgraph verification errors with precise pin, net and passive components value error.
- **Concise error messages:** Contains only the error type without detailed pin/net information.
- **Binary:** Provides only a pass or fail status only.

Mirroring expert practices, we implement a subcircuit reuse strategy. Validated modules from simpler tasks populate a library, which the LLM retrieves to synthesize complex hierarchical or planar designs. Ablation studies confirm that this retrieval mechanism significantly enhances success rates.

4. Experiments

4.1. Experiment Setup

We evaluate existing LLMs ability for understanding the pin functions, KG, and topology constrains, the topology generation capability, and analog/digital/power mixed domain synthesis capability. We widely employed most of state-of-the-art LLMs, including DeepSeek-V3.2 (DeepSeek-AI et al., 2024), Llama 3 and Llama 4 (Dubey et al., 2024; Meta, 2025), MiniMax M2.1 (Minimax, 2025), Qwen 3 Max (Yang et al., 2025), GPT 5.1 (OpenAI, 2025), and Gemini 3 series (Google DeepMind, 2025a;b). To address some potential confidential PCB requirements (e.g. Milliary and Academic Research), we further evaluated open-source LLMs, such as Llama 3 & 4 series (Dubey et al., 2024; Meta, 2025) and GPT-OSS for potential locally-hosted applications. All models temperature are set as 0.5. We also fine-tuned GPT-4o-mini model for ablation studies.

Evaluation Metrics: We use most common *Pass@k* metrics for code generation evaluation (Chen et al., 2021). The *Pass@k* measures the probability of achieving at least one success within k independent trials, where each trial allows for a maximum of three self-correction retry attempts. We perform n trials where $n > k$, and count the metric as $\text{Pass}@k = 1 - \frac{\binom{n-c}{k}}{\binom{n}{k}}$, where c denotes the number of successful trials. We set k to be 1 and 5 for single-shot reliability and robustness. We set n to be 15 for all experiments. We further justify our sample size in the Appendix by plotting 95% confidence intervals for $n = 15$, confirming that the results are statistically robust.

Data Preparation: As this task targets at PCB schematic generation via real-world IC components, we constructed the benchmark and component library based on real-world IC datasheets. Furthermore, we want to check if LLM fully understand the functionality of the IC chips. We also injected a few components with same package and similar pin numbers but different functionality (e.g. voltage regulator vs. op-amp) to check if LLM can distinguish them and choose correct components. The details of the component library construction is provided in Appendix.

Benchmark. We developed a comprehensive benchmark of PCB schematic design tasks with analog, digital and power circuits, as well as mix of them. The benchmark consists of 23 unique tasks, each associated with real-world IC components and datasheets. The benchmark tasks summary is provided in Table 1. The difficulty levels are depended on circuit nodes and nets numbers, ranging from 4 component pins to over 100 component pins. The benchmark details are summarized in Appendix.

4.2. Main Results

Results Analysis: We applied our Constraint-Guided Schematic Design framework with all LLMs for efficiently evaluate LLMs performance. Our experimental evaluation incorporates all the strategies discussed in Section 3, including prompt engineering including ICL and CoT, multi-stage verification and feedback strategy as well as subcircuit library reuse. The main results are summarized in Table 2. The results demonstrate that our proposed **PCBSchemaGen** framework significantly enhances the schematic generation capabilities of various LLMs. Experimental results show that, on certain problems, state-of-the-art open-source models can be competitive with GPT-5.1 (OpenAI, 2025) in PCB schematic generation, e.g., DeepSeek-V3.2 (DeepSeek-AI et al., 2024) and GPT-OSS_120B. For instance, on easy-level tasks, they can all ensure Pass@5 robustness. On medium-level tasks, DeepSeek-V3.2 (DeepSeek-AI et al., 2024) also achieves a success rate close to that of GPT-5.1 (OpenAI, 2025) (e.g., Task 12: QFN power stage; and Task 15: isolated gate driver). Overall, however, open-source models still under perform closed-source models on complex tasks, i.e. when the design contains large component network with more than 20 devices and 70 device pins.

Beyond accuracy, we evaluated the operational cost of our framework. For the best cost efficient model, the average consumption per task is approximately **23k** tokens, translating to a cost of **0.07 USD** and a runtime of roughly **2.4 minutes**. In contrast, a human expert typically requires **1.5 hours** for similar schematic designs. This represents $\approx 37 \times$ **speedup**, demonstrating that PCBSchemaGen offers a highly time-efficient solution for board-level design automation. We attribute this gap to the fact that complex

Table 1. Summary of PCBSchemaGen benchmark tasks (ID 1–23).

ID	Type	Task Summary	ID	Type	Task Summary
1	Sensing	Resistor divider for HV-to-LV ADC sensing.	13	Driver	Low-side gate driver with gate resistor.
2	Sensing	Isolated voltage sensing with AMC1350.	14	Driver	Bootstrap HB gate driver with integrated diode.
3	Sensing	Diff-to-SE amplifier with VREF offset.	15	Driver	Isolated gate driver with bipolar supply.
4	Sensing	Hall-effect isolated current sensing.	16	Driver	Protected isolated driver (DESAT, Miller clamp).
5	AuxPower	LDO-based regulated low-voltage supply.	17	DC-DC	Synchronous buck converter with full control.
6	AuxPower	Low voltage auxiliary buck regulator.	18	DC-DC	Synchronous boost converter with full control.
7	AuxPower	Isolated DC-DC for gate-drive rails.	19	DC-DC	4-switch buck-boost converter using two HBs.
8	PowerStage	TO-247-3 MOSFET half-bridge power stage.	20	DC-DC	Dual active bridge (DAB) with full bridges.
9	PowerStage	TO-247-3 MOSFET half-bridge power stage.	21	DC-DC	LLC resonant converter with isolated output.
10	PowerStage	TOLL MOSFET HB stage (Kelvin source).	22	DC-AC	3-phase motor drive using three HBs.
11	PowerStage	TOLT top-side-cooled MOSFET HB stage.	23	DC-AC	Single-phase grid-tied inverter from DC link.
12	PowerStage	QFN-8×8 integrated half-bridge power stage.			

Table 2. Main results (updated with our experiments). Models are sorted left-to-right by overall Pass@1 (worst → best). Pass@1 and Pass@5 are computed from $n = 15$ trials per task using $\widehat{\text{pass@}k} = 1 - \binom{n-c}{k} / \binom{n}{k}$.

Model Task ID	Llama3-70B Pass@1	Llama3-70B Pass@5	Llama-4-Maverick Pass@1	Llama-4-Maverick Pass@5	MiniMax-M2.1 Pass@1	MiniMax-M2.1 Pass@5	Qwen3-Max Pass@1	Qwen3-Max Pass@5	GPT-OS-120B Pass@1	GPT-OS-120B Pass@5	DeepSeek-V3.2 Pass@1	DeepSeek-V3.2 Pass@5	GPT-5.1 Pass@1	GPT-5.1 Pass@5	Gemini-3-Flash Pass@1	Gemini-3-Flash Pass@5	Gemini-3-Pro Pass@1	Gemini-3-Pro Pass@5
1	100.0	100.0	53.3	99.3	100.0	100.0	100.0	100.0	93.3	100.0	100.0	100.0	100.0	100.0	100.0	100.0	100.0	100.0
2	100.0	100.0	100.0	100.0	93.3	100.0	100.0	100.0	100.0	100.0	100.0	100.0	100.0	100.0	100.0	100.0	100.0	
3	0.0	0.0	26.7	84.6	46.7	98.1	40.0	95.8	53.3	99.3	46.7	98.1	100.0	100.0	73.3	100.0	100.0	100.0
4	60.0	99.8	46.7	98.1	80.0	100.0	20.0	73.6	20.0	73.6	73.3	100.0	100.0	100.0	100.0	100.0	86.7	100.0
5	86.7	100.0	93.3	100.0	100.0	100.0	100.0	100.0	100.0	100.0	100.0	100.0	100.0	100.0	100.0	100.0	100.0	
6	26.7	84.6	100.0	100.0	86.7	100.0	93.3	100.0	86.7	100.0	100.0	100.0	100.0	100.0	86.7	100.0	100.0	100.0
7	26.7	84.6	60.0	99.8	73.3	100.0	100.0	100.0	100.0	100.0	93.3	100.0	100.0	100.0	100.0	100.0	100.0	100.0
8	20.0	73.6	93.3	100.0	100.0	100.0	100.0	100.0	93.3	100.0	100.0	100.0	93.3	100.0	100.0	100.0	100.0	100.0
9	40.0	95.8	40.0	95.8	6.7	33.3	66.7	100.0	60.0	99.8	86.7	100.0	53.3	99.3	100.0	100.0	100.0	100.0
10	0.0	0.0	13.3	57.1	0.0	0.0	46.7	98.1	40.0	95.8	33.3	91.6	40.0	95.8	100.0	100.0	100.0	100.0
11	0.0	0.0	0.0	0.0	40.0	95.8	33.3	91.6	46.7	98.1	66.7	100.0	46.7	98.1	100.0	100.0	100.0	100.0
12	0.0	0.0	0.0	0.0	13.3	57.1	0.0	0.0	73.3	100.0	93.3	100.0	86.7	100.0	93.3	100.0	93.3	100.0
13	13.3	57.1	53.3	99.3	66.7	100.0	86.7	100.0	66.7	100.0	86.7	100.0	93.3	100.0	100.0	100.0	100.0	100.0
14	86.7	100.0	66.7	100.0	100.0	100.0	100.0	100.0	100.0	100.0	100.0	100.0	100.0	100.0	100.0	100.0	100.0	100.0
15	46.7	98.1	86.7	100.0	86.7	100.0	100.0	100.0	100.0	100.0	100.0	100.0	100.0	100.0	100.0	100.0	100.0	100.0
16	0.0	0.0	0.0	0.0	0.0	0.0	0.0	0.0	13.3	57.1	0.0	0.0	86.7	100.0	33.3	91.6	60.0	99.8
# Solved	11	11	15	15	19	19	17	17	20	20	21	21	22	22	22	22	22	22
Overall Pass@1 (%)	26.4	—	37.4	—	48.7	—	51.3	—	60.0	—	73.0	—	83.2	—	88.1	—	86.1	—

tasks require not only stronger reasoning and knowledge retrieval/integration for individual devices, but also more robust abstraction over circuit connectivity, spatial reasoning, and circuit-level conceptualization. Consequently, strong domain expertise, general reasoning, and spatial reasoning capabilities are critical for LLMs in this setting. In our experiments, Gemini 3 series (Google DeepMind, 2025a;b) achieves the best overall performance, which we suspect partly due to its (claimed) stronger multi-modal capabilities that may benefit circuit-topology understanding.

Baselines: Comparing against GNN (Plettenberg et al., 2025) and LLM (Hasan et al., 2026) (aligned by component/pin counts), our framework achieves substantially higher success rates. Full comparative details are provided in the Appendix.

Table 3. Comparison with baselines. Our framework significantly outperforms others.

Task Complexity	Ours (Full)	CircuitLM (Hasan et al., 2026)	GNN (Plettenberg et al., 2025)
Easy (< 10 pins)	93.3%	53.0%	80%
Medium (10 ~ 50)	92.7%	N/A	N/A
Hard (> 100 pins)	78.1%	N/A	N/A

Example of Result Details: In the subsequent figures, we use Task 3 and Task 11 as representative examples to visualize successful and failed designs. Beyond syntax and code errors, the most common failure modes are (i) misunderstanding the function of a specific pin, and (ii) generating meaningless connections due to an inability to correctly synthesize the abstract circuit topology. In task 3, we designed the task to build a differential to single-end op-amp buffer that converts the differential analog voltage into single-end voltage signal. Input pair peak voltage $V_{in} = V_{in+} - V_{in-} = 2V$, output voltage $V_{out} = 3V$ and supply voltage $V_{cc} = 3.3V$. So the generated circuit not only should contain four resistors such that the circuit structure connection should be differential to single-end semantics, the LLM also should set resistor values correct such that $V_{out} = (V_{in+} \times \frac{R4}{R3} - V_{in-} \times \frac{R1}{R2}) + V_{ref}$. In task 11, the task is to build a Silicon-Carbide (SiC) based 650V MOSFETs half-bridges with High-Frequency (HF) capacitors to enhance its transient switching performance. The LLM should learn from the component information injection that pin "KS" refers to Kelvin-Source especially designed for high-voltage high-power MOSFETs (This pin

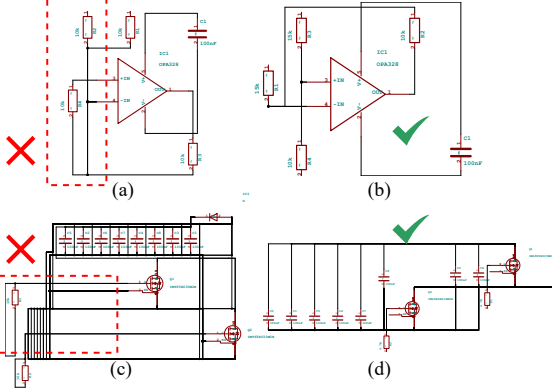


Figure 4. Visualizations of generated PCB schematics. (a) Task #3 failure (wrong op-amp feedback R_1, R_2, R_4) vs. (b) correct output. (c) Task #11 failure (mis-connected Kelvin-Source) vs. (d) correct output.

is scarce in conventional SPICE simulation, which most of Analog circuit code generation works rely on). The LLM should learn the correct connection of KS as well as the gate resistor values.

4.3. Ablation Studies

Feedback Level: To validate our verification loop, we ablated feedback strength: *Full* (type and location), *Weak* (type only), and *None* (binary). Table 4 shows that while simple tasks are insensitive, *Full* feedback is indispensable for complex designs, where explicit localization enables precise self-correction and significantly boosts success.

Table 4. Impact of feedback granularity. Full feedback with error localization yields the highest success rates, particularly in Medium and Hard tasks.

Difficulty	Gemini-3-Flash (Full)	Gemini-3-Flash (Weak)	Gemini-3-Flash (None)
Easy (P1-P6)	93.3%	91.1%	85.6%
Medium (P7-P16)	92.7%	58.0%	58.0%
Hard (P17-P23)	78.1%	68.6%	57.1%

Table 5. Ablation on prompting strategies. ICL proves essential for complex designs, maintaining performance where zero-shot approaches fail (78.1% \rightarrow 43.8% in Hard tasks).

Difficulty	Gemini-3-Flash (Full)	Gemini-3-Flash (No ICL)	Gemini-3-Flash (No CoT)
Easy (P1-P6)	93.3%	95.6%	86.7%
Medium (P7-P16)	92.7%	92.0%	82.0%
Hard (P17-P23)	78.1%	43.8%	75.2%

Prompt Techniques: Table 5 validates the critical role of prompt engineering strategies. While basic prompting suffices for *Easy* tasks (where removing ICL marginally reduces context noise), **ICL is indispensable for scalability**: removing it in *Hard* tasks triggers a performance collapse

(78.1% \rightarrow 43.8%), confirming that structural exemplars are vital for complex synthesis. Additionally, removing CoT consistently degrades performance across all levels, underscoring its necessity for logical reasoning stability.

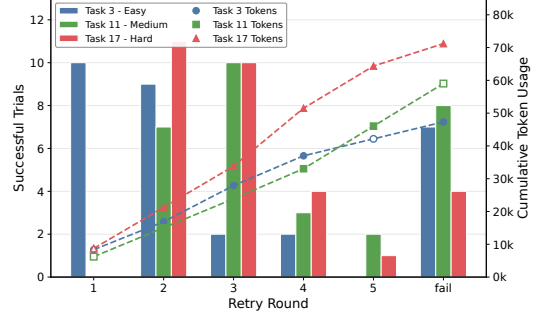


Figure 5. Success distribution and cumulative token usage across retry rounds.

Number of Retry: Fig. 5 contrasts linear token growth (lines) with success distribution (bars). Since most valid designs emerge within the first three iterations, we cap retries at three to avoid diminishing returns and token wast.

4.4. Human Experts Evaluation

To assess our multi-stage verification completeness, an independent human expert (Ph.D., >10 years PCB design experience) conducted a blind review of 460 stratified samples. The resulting Cohen's Kappa (κ) (Cohen, 1960; Landis & Koch, 1977) coefficients demonstrate robust alignment across all difficulty levels: 0.95 (Easy), 0.89 (Medium), and 0.913 (Hard), yielding an overall κ of 0.913. These values fall well within the high-confidence interval, confirming the proposed verifier's great validity. The detailed confusion matrix is presented in Appendix.

5. Conclusion

We presented PCBSchemaGen, the first training-free framework for PCB schematic automation. By anchoring LLM synthesis in a datasheet-driven Knowledge Graph verifier, we effectively address data scarcity and the lack of universal simulators. Experiments on 23 benchmarks demonstrate that enforcing real-world IC constraints significantly enhances accuracy. This work bridges the gap between functional intent and physical implementation, establishing a robust foundation for future hardware automation.

Impact Statement

This paper presents work whose goal is to advance the field of Machine Learning for Electronic Design Automation. Our proposed knowledge-graph-driven verification pipeline ensures electrical correctness of generated circuits through

formal constraints, contributing to improved reliability and efficiency in circuit design. There are many potential societal consequences of our work, none which we feel must be specifically highlighted here.

References

Amano, H., Baines, Y., Beam, E., et al. The 2018 gan power electronics roadmap. *Journal of Physics D: Applied Physics*, 51(16):163001, April 2018. ISSN 0022-3727, 1361-6463. doi: 10.1088/1361-6463/aaaf9d.

Bhandari, J., Bhat, V., He, Y., Rahmani, H., Garg, S., and Karri, R. Masala-chai: A large-scale spice netlist dataset for analog circuits by harnessing ai, 2024.

Blocklove, J., Garg, S., Karri, R., and Pearce, H. Chip-chat: Challenges and opportunities in conversational hardware design. In *2023 ACM/IEEE 5th Workshop on Machine Learning for CAD (MLCAD)*, pp. 1–6, Snowbird, UT, USA, September 2023. IEEE. ISBN 979-8-3503-0955-3. doi: 10.1109/MLCAD58807.2023.10299874.

Chang, C.-C., Lin, W.-H., Shen, Y., Chen, Y., and Zhang, X. Lamagic2: Advanced circuit formulations for language model-based analog topology generation, 2025.

Chen, M., Tworek, J., Jun, H., et al. Evaluating large language models trained on code, 2021. URL <https://arxiv.org/abs/2107.03374>.

Chen, X., Lin, M., Schärli, N., and Zhou, D. Teaching large language models to self-debug, 2023.

Chen, Z., Huang, J., Liu, Y., Yang, F., Shang, L., Zhou, D., and Zeng, X. Artisan: Automated operational amplifier design via domain-specific large language model. In *Proceedings of the 61st ACM/IEEE Design Automation Conference*, pp. 1–6, San Francisco CA USA, June 2024. ACM. ISBN 979-8-4007-0601-1. doi: 10.1145/3649329.3655903.

Cohen, J. A coefficient of agreement for nominal scales. *Educational and psychological measurement*, 20(1):37–46, 1960.

Cordella, L. P., Foggia, P., Sansone, C., and Vento, M. A (sub) graph isomorphism algorithm for matching large graphs. *IEEE transactions on pattern analysis and machine intelligence*, 26(10):1367–1372, 2004.

DeepSeek-AI, Liu, A., Feng, B., et al. Deepseek-v3 technical report, 2024.

DeLorenzo, M., Chowdhury, A. B., Gohil, V., Thakur, S., Karri, R., Garg, S., and Rajendran, J. Make every move count: Llm-based high-quality rtl code generation using mcts, 2024.

Dong, Q., Li, L., Dai, D., Zheng, C., Ma, J., Li, R., Xia, H., Xu, J., Wu, Z., Liu, T., Chang, B., Sun, X., and Sui, Z. A survey on in-context learning, 2023a.

Dong, Z., Cao, W., Zhang, M., Tao, D., Chen, Y., and Zhang, X. Cktgnn: Circuit graph neural network for electronic design automation, 2023b.

Dubey, A., Jauhri, A., Pandey, A., Kadian, A., Al-Dahle, A., Letman, A., Mathur, A., Schelten, A., Yang, A., Fan, A., et al. The llama 3 herd of models. *arXiv e-prints*, pp. arXiv–2407, 2024.

Fortune Business Insights. Printed circuit board market size, share & industry analysis, by product type (rigid board (single layer board, double layer board, and others (multilayer)), hdi board, flexible board, and others), by application (automotive, consumer electronics, telecommunication, healthcare, energy & power, and others (military, utilities)), and regional forecast, 2025–2032. <https://www.fortunebusinessinsights.com/printed-circuit-board-market-104947>, 2026. Accessed: 2026-01-27.

Fu, Y., Zhang, Y., Yu, Z., Li, S., Ye, Z., Li, C., Wan, C., and Lin, Y. C. Gpt4aigchip: Towards next-generation ai accelerator design automation via large language models. In *2023 IEEE/ACM International Conference on Computer Aided Design (ICCAD)*, pp. 1–9, San Francisco, CA, USA, October 2023. IEEE. ISBN 979-8-3503-2225-5. doi: 10.1109/ICCAD57390.2023.10323953.

Gao, J., Cao, W., and Zhang, X. Analoggenie-lite: Enhancing scalability and precision in circuit topology discovery through lightweight graph modeling. In *Forty-second International Conference on Machine Learning*.

Gao, J., Cao, W., Yang, J., and Zhang, X. Analoggenie: A generative engine for automatic discovery of analog circuit topologies, 2025.

Google DeepMind. Gemini 3 Flash – model card. Model card (PDF), December 2025a. URL <https://deephind.google/models/model-cards/gemini-3-flash/>. Published: December 2025. Accessed: 2026-01-27.

Google DeepMind. Gemini 3 Pro – model card. Model card (PDF), November 2025b. URL <https://deephind.google/models/model-cards/gemini-3-pro/>. Published/Model release: November 2025. Accessed: 2026-01-27.

Hasan, K. S. A., Raiyan, S. R., Alvee, H. M., and Sadik, W. Circuitlm: A multi-agent llm-aided design framework for generating circuit schematics from natural language prompts, 2026. URL <https://arxiv.org/abs/2601.04505>.

Hong, S., Zhuge, M., Chen, J., Zheng, X., Cheng, Y., Zhang, C., Wang, J., Wang, Z., Yau, S. K. S., Lin, Z., Zhou, L., Ran, C., Xiao, L., Wu, C., and Schmidhuber, J. Metagpt: Meta programming for a multi-agent collaborative framework, 2023.

Huang, A. Q., Crow, M. L., Heydt, G. T., Zheng, J. P., and Dale, S. J. The future renewable electric energy delivery and management (freedm) system: The energy internet. *Proceedings of the IEEE*, 99(1):133–148, January 2011. ISSN 0018-9219, 1558-2256. doi: 10.1109/JPROC.2010.2081330.

Jin, H., Wang, J., Sheng, J., Wu, Y., Chen, J., Wang, Y., and Liu, J. Wiseeda: Llms in rf circuit design. *Microelectronics Journal*, 158:106607, 2025. ISSN 1879-2391. doi: <https://doi.org/10.1016/j.mejo.2025.106607>. URL <https://www.sciencedirect.com/science/article/pii/S1879239125000566>.

Kim, D.-H., Lu, N., Ma, R., Kim, Y.-S., Kim, R.-H., Wang, S., Wu, J., Won, S. M., Tao, H., Islam, A., et al. Epidermal electronics. *science*, 333(6044):838–843, 2011.

Kumar Jha, S., Jha, S., Haq Rashed, M. R., Ewetz, R., and Velasquez, A. Automated synthesis of hardware designs using symbolic feedback and grammar-constrained decoding in large language models. In *NAECON 2024 - IEEE National Aerospace and Electronics Conference*, pp. 95–100, 2024. doi: 10.1109/NAECON61878.2024.10670630.

Lai, Y., Liu, J., Tang, Z., Wang, B., Hao, J., and Luo, P. Chipformer: Transferable chip placement via offline decision transformer, 2023.

Lai, Y., Lee, S., Chen, G., Poddar, S., Hu, M., Pan, D. Z., and Luo, P. Analogcoder: Analog circuit design via training-free code generation. *Proceedings of the AAAI Conference on Artificial Intelligence*, 39(1):379–387, April 2025. ISSN 2374-3468, 2159-5399. doi: 10.1609/aaai.v39i1.32016.

Landis, J. R. and Koch, G. G. The measurement of observer agreement for categorical data. *biometrics*, pp. 159–174, 1977.

Li, H., Zhang, J., Xu, N., and Liu, M. Fanoutnet: A neuralized pcb fanout automation method using deep reinforcement learning. *Proceedings of the AAAI Conference on Artificial Intelligence*, 37(7):8554–8561, June 2023. ISSN 2374-3468, 2159-5399. doi: 10.1609/aaai.v37i7.26030.

Li, M., Fang, W., Zhang, Q., and Xie, Z. Specllm: Exploring generation and review of vlsi design specification with large language model, 2024.

Lin, F., Li, X., Lei, W., Rodriguez-Andina, J. J., Guerrero, J. M., Wen, C., Zhang, X., and Ma, H. Pe-gpt: A new paradigm for power electronics design. *IEEE Transactions on Industrial Electronics*, 72(4):3778–3791, April 2025. ISSN 0278-0046, 1557-9948. doi: 10.1109/TIE.2024.3454408.

Liu, B., Zhang, H., Gao, X., Kong, Z., Tang, X., Lin, Y., Wang, R., and Huang, R. Layoutcopilot: An llm-powered multi-agent collaborative framework for interactive analog layout design, 2024a.

Liu, C. and Chitnis, D. Eeschematic: Multimodal-llm based ai agent for schematic generation of analog circuit, 2025. URL <https://arxiv.org/abs/2510.17002>.

Liu, C., Chen, W., Peng, A., Du, Y., Du, L., and Yang, J. Am-pagent: An llm-based multi-agent system for multi-stage amplifier schematic design from literature for process and performance porting, 2024b.

Liu, M., Ene, T.-D., Kirby, R., et al. Chipnemo: Domain-adapted llms for chip design, 2023a.

Liu, M., Pinckney, N., Khailany, B., and Ren, H. Verilogeval: Evaluating large language models for verilog code generation, 2023b.

Liu, Y., Xu, C., Zhou, Y., Li, Z., and Xu, Q. Deeprtl: Bridging verilog understanding and generation with a unified representation model, 2025.

Lu, P., Bansal, H., Xia, T., Liu, J., Li, C., Hajishirzi, H., Cheng, H., Chang, K.-W., Galley, M., and Gao, J. Math-vista: Evaluating mathematical reasoning of foundation models in visual contexts. In *International Conference on Learning Representations (ICLR)*, 2024.

Matsuo, R., Uhlich, S., Venkitaraman, A., Bonetti, A., Hsieh, C.-Y., Momeni, A., Mauch, L., Capone, A., Ohbuch, E., and Servadei, L. Schemato – an llm for netlist-to-schematic conversion, 2024.

Meta. The llama 4 herd: The beginning of a new era of natively multimodal AI innovation, April 2025. URL <https://about.fb.com/ja/news/2025/04/llama-4-multimodal-intelligence/>. Meta Newsroom post announcing Llama 4 Scout and Llama 4 Maverick.

MiniMax. MiniMax M2.1: Significantly enhanced multi-language programming, built for real-world complex tasks, December 2025. URL <https://www.minimax.io/news/minimax-m21>. Mini-Max News release post.

Mirhoseini, A., Goldie, A., Yazgan, M., et al. A graph placement methodology for fast chip design. *Nature*, 594

(7862):207–212, June 2021. ISSN 0028-0836, 1476-4687. doi: 10.1038/s41586-021-03544-w.

Olausson, T. X., Inala, J. P., Wang, C., Gao, J., and Solar-Lezama, A. Is self-repair a silver bullet for code generation?, 2023.

OpenAI. Introducing GPT-5.1, November 2025. URL <https://academy.openai.com/home/resources/intro-gpt-5-1>. OpenAI Academy resource (published 2025-11-21).

Pan, J., Jacobson, I., Zhao, Z., Chen, T.-C., Zhou, G., Chang, C.-C., Rashingkar, V., and Chen, Y. Crop: Circuit retrieval and optimization with parameter guidance using llms, 2025. URL <https://arxiv.org/abs/2507.02128>.

Pecht, M. Prognostics and health management of electronics. *Encyclopedia of structural health monitoring*, 2009.

Pei, Z., Zhen, H.-L., Yuan, M., Huang, Y., and Yu, B. Betterv: Controlled verilog generation with discriminative guidance, 2024.

Plettenberg, P., Alcalde, A., Sick, B., and Thomas, J. M. Graph neural networks for automatic addition of optimizing components in printed circuit board schematics. In *Joint European Conference on Machine Learning and Knowledge Discovery in Databases*, pp. 508–524. Springer, 2025.

Qin, Y., Liang, S., Ye, Y., Zhu, K., Yan, L., Lu, Y., Lin, Y., Cong, X., Tang, X., Qian, B., Zhao, S., Hong, L., Tian, R., Xie, R., Zhou, J., Gerstein, M., Li, D., Liu, Z., and Sun, M. Toolllm: Facilitating large language models to master 16000+ real-world apis, 2023.

Shi, Y., Tao, Z., Gao, Y., Zhou, T., Chang, C., Wang, Y., Chen, B., Zhang, G., Liu, A., Yu, Z., Lin, T.-J., and He, L. Amsnet-kg: A netlist dataset for llm-based ams circuit auto-design using knowledge graph rag. *ACM Transactions on Design Automation of Electronic Systems*, 30(6):1–37, November 2025. ISSN 1084-4309, 1557-7309. doi: 10.1145/3736166.

Thakur, S., Blocklode, J., Pearce, H., Tan, B., Garg, S., and Karri, R. Autochip: Automating hdl generation using llm feedback, 2023.

Thakur, S., Ahmad, B., Pearce, H., Tan, B., Dolan-Gavitt, B., Karri, R., and Garg, S. Verigen: A large language model for verilog code generation. *ACM Transactions on Design Automation of Electronic Systems*, 29(3):1–31, May 2024. ISSN 1084-4309, 1557-7309. doi: 10.1145/3643681.

Thomas, D. E. and Moorby, P. R. *The Verilog® Hardware Description Language*. Springer US, Boston, MA, 2002. ISBN 978-0-387-84930-0. doi: 10.1007/978-0-387-85344-4.

Vandenboud, D. Skidl: A python package for textually describing electronic circuit schematics, December 2025. URL <https://pypi.org/project/skidl/>. PyPI project page and release history.

Vijayaraghavan, P., Shi, L., Degan, E., Mukherjee, V., and Zhang, X. Circuitsynth-rl: Llm-based circuit topology synthesis with rl refinement. In *ACM/IEEE Design Automation Conference*, 2025a.

Vijayaraghavan, P., Shi, L., Degan, E., Mukherjee, V., and Zhang, X. Autocircuit-rl: Reinforcement learning-driven llm for automated circuit topology generation, 2025b.

Wang, X., Han, B., Tai, Z., Tian, J., Wang, Y., Yan, J., and Tian, Y. New interaction paradigm for complex eda software leveraging gpt, 2023.

Wang, Y., Lu, T., Liu, R., Yang, L., Yang, Y., Chen, Z., Wang, Y., Liu, Y., Lin, K., Chen, X., et al. A large language model powered integrated circuit footprint geometry understanding. *arXiv preprint arXiv:2508.03725*, 2025.

Wei, J., Wang, X., Schuurmans, D., Bosma, M., Ichter, B., Xia, F., Chi, E., Le, Q., and Zhou, D. Chain-of-thought prompting elicits reasoning in large language models, 2023. URL <https://arxiv.org/abs/2201.11903>.

Wei, Z., Kong, Z., Wang, Y., Pan, D. Z., and Tang, X. Toposizing: An llm-aided framework of topology-based understanding and sizing for ams circuits, 2025.

Wu, H., He, Z., Zhang, X., Yao, X., Zheng, S., Zheng, H., and Yu, B. Chateda: A large language model powered autonomous agent for eda. *IEEE Transactions on Computer-Aided Design of Integrated Circuits and Systems*, 43(10):3184–3197, October 2024. ISSN 0278-0070, 1937-4151. doi: 10.1109/TCAD.2024.3383347.

Yan, J., Norman, A., Lim, M. S., Norman, M., Ho, H. C., Zhu, J., and MA, M. Ai-based floorplanning for printed circuit board design, September 22 2022. US Patent App. 17/835,323.

Yang, A., Li, A., Yang, B., et al. Qwen3 technical report, 2025.

Yin, Y., Wang, Y., Xu, B., and Li, P. Ado-llm: Analog design bayesian optimization with in-context learning of large language models. In *Proceedings of the 43rd IEEE/ACM International Conference on Computer-Aided Design*, pp. 1–9, Newark Liberty International Airport Marriott New York NY USA, October 2024. ACM. ISBN 979-8-4007-1077-3. doi: 10.1145/3676536.3676816.

Zhang, K., Zhang, H., Li, A., Yang, Z., and Chu, X. Applying existing large language models for print circuit board routing. In *ICSEE 2024*, pp. 2. MDPI, February 2025a. doi: 10.3390/engproc2025086002.

Zhang, R., Wen, Y., Cheng, S., Huang, D., Peng, S., Guo, J., Jin, P., Zhao, J., Ma, T., Zhu, Y., et al. Qimeng: Fully automated hardware and software design for processor chip. *arXiv preprint arXiv:2506.05007*, 2025b.

Zhang, Y., Zhang, R., Guo, J., Huang, L., Huang, D., Zhao, Y., Cheng, S., Jin, P., Li, C., Du, Z., Hu, X., Guo, Q., and Chen, Y. Qimeng-salv: Signal-aware learning for verilog code generation, 2025c.

Zhu, Y., Huang, D., Lyu, H., Zhang, X., Li, C., Shi, W., Wu, Y., Mu, J., Wang, J., Zhao, Y., Jin, P., Cheng, S., Liang, S., Zhang, X., Zhang, R., Du, Z., Guo, Q., Hu, X., and Chen, Y. Qimeng-codev-r1: Reasoning-enhanced verilog generation, 2025.

A. Appendix

Road map:

In Appendix section, we provide detailed benchmark task list in [A.1](#), then we list the comprehensive prompts for easy/medium level tasks and hard level tasks in [A.2](#) and [A.3](#). [A.4](#) propose formalization of verification stages and feedback loop, and [A.5](#) is example of multi-stage verification process. [A.6](#) to [A.9](#) provide other essential technical details. [A.10](#) provide math prove for confidence interval, and [A.11](#) provide human expert evaluation result. [A.12](#) to [A.15](#) provide extensive ablation studies and discussion. [A.16](#) provide detailed failed sample analysis.

A.1. Benchmark Task List Detail

Table 6 provides the comprehensive list of the 23 design tasks used in our evaluation, categorized by difficulty level and circuit type.

Table 6. Detailed specifications of the PCBSchemaGen benchmark tasks.

ID	Level	Type	Design Task Description	I/O Nodes	V/I Level	Key Components
1	Easy	Analog Sensing	A resistor divider to scale a high-voltage input to a low-voltage sense node for single-end ADC measurement.	VIN → VSENSE	60V → 3.3V	Resistors
2	Easy	Analog Sensing	An isolated voltage sensing front-end using a resistor divider with an isolated amplifier to measure a high-voltage bus and output an isolated differential low-voltage sense signal.	VIN → OUTP, OUTN	400V → 3.3V	AMC1350 (Iso-Amp)
3	Easy	Analog Sensing	A differential-to-single-ended amplifier using one op-amp with a VREF offset. Assume VREF=1.65V and differential input VINP-VINN = ±2.0V.	VINP, VINN → VOUT	2V → 3V	OPA328 (Op-Amp)
4	Easy	Analog Sensing	A Hall-effect isolated current sensing circuit that measures line current through an integrated isolated current path and outputs an isolated analog signal.	LINE_IN → ISNS_ISO	50A → 3.3V	ACS37010 (Hall Sensor)
5	Easy	Auxiliary Power	An LDO-based supply that converts a DC input into a regulated low-voltage rail.	VIN → VOUT	12V → 3.3V	TLV1117-33 (LDO)
6	Easy	Auxiliary Power	A low voltage auxiliary buck regulator using chip that converts a DC input into a regulated low-voltage rail.	VIN → VOUT	12V → 3.3V	TPS54302 (Buck)
7	Medium	Auxiliary Power	An isolated DC-DC module that generates isolated positive and negative gate-drive supply rails for isolated gate drivers or sensors.	VIN → VISO+, VISO-	12V → 15V, -9V	MGJ2D121505 (Iso-DCDC)
8	Medium	High Power Stage	A TO-247-3 MOSFET half-bridge power stage with a switching phase output. Includes at least 8 decoupling caps for high dv/dt loop.	VBUS+ → VSW	400V → 400V	IMW65R015M2H (SiC FET)
9	Medium	High Power Stage	A TO-247-4 SiC MOSFET half-bridge stage with Kelvin source connection and 8 decoupling capacitors.	VBUS+ → VSW	400V → 400V	IMZA65R015M2H (SiC FET)
10	Medium	Power Stage	A TOLL MOSFET half-bridge stage with Kelvin source connection and 8 decoupling capacitors.	VBUS+ → VSW	400V → 400V	IMT65R033M2H (SiC FET)
11	Medium	High Power Stage	A TOLT top-side-cooled MOSFET half-bridge stage with Kelvin source connection and 8 decoupling capacitors.	VBUS+ → VSW	400V → 400V	IMLT65R015M2H (SiC FET)
12	Medium	Power Stage	A QFN-8*8 integrated half-bridge power stage with 8 decoupling capacitors.	VBUS+ → VSW	48V → 48V	BSC052N08NS5 (MOSFET)
13	Medium	Gate Driver	A low-side gate driver that drives a MOSFET gate from a logic-level PWM signal, including gate resistor.	PWM, VCC → GATE	9V → 12V	UCC27511 (Driver)
14	Medium	Gate Driver	A bootstrap high-side/low-side half-bridge gate driver with integrated bootstrap diode and gate resistors.	PWM_H, L → HO, LO	12V → 12V	UCC27211 (HB Driver)
15	Medium	Gate Driver	An isolated gate driver with secondary side driven by isolated bipolar +15/-9V power supply.	PWM, VCC → OUT	3.3V → 15V/-9V	UCC5390E (Iso-Driver)
16	Medium	Gate Driver	A protected isolated gate driver with DESAT detection, Miller clamp, fault reporting, and enable control.	PWM, VCC → OUT, FLT	5V → 15V/-9V	UCC21710 (Iso-Driver)
17	Hard	DC-DC Converter	A synchronous buck converter using a half-bridge power stage. Include gate drivers with individual turn-on/off speed control and power supply.	VIN, PWM → VOUT	200V → 100V	IMZA65R015M2H (SiC FET)
18	Hard	DC-DC Converter	A synchronous boost converter using a half-bridge power stage. Include gate drivers with individual turn-on/off speed control and power supply.	VIN, PWM → VOUT	100V → 200V	IMZA65R015M2H (SiC FET)
19	Hard	DC-DC Converter	A 4-switch buck-boost converter using two half-bridges. Include gate drivers with individual turn-on/off speed control and power supply.	VIN, PWM → VOUT	200V → 200V	IMZA65R015M2H (SiC FET)
20	Hard	DC-DC Converter	A dual active bridge (DAB) converter with full bridges, blocking caps, and external inductors. Include gate drivers and power supply.	VIN, PWM → VSW	400V → 400V	IMZA65R015M2H (SiC FET)
21	Hard	DC-DC Converter	An LLC resonant converter with an isolated transformer output, blocking caps, and external inductors. Include gate drivers and power supply.	VIN, PWM → VSW	400V → 12V	IMZA65R015M2H (SiC FET)
22	Hard	DC-AC Converter	A 3-phase motor drive using three half-bridges. Include gate drivers with individual turn-on/off speed control and power supply.	VIN, PWM → VSW	400V → 230V	IMZA65R015M2H (SiC FET)
23	Hard	DC-AC Converter	A single-phase grid-tied inverter from a DC link input. Include gate drivers with individual turn-on/off speed control and power supply.	VIN, PWM → VSW	400V → 230V	IMZA65R015M2H (SiC FET)

A.2. Complete Prompts for Easy & Medium Level Tasks

User Prompt

You aim to design a PCB schematic using SKiDL (Python) for a given circuit described in the text.

Please ensure your designed circuit works properly, satisfies the requirements, and follows specific library conventions.

Assistant Prompt (For Non-hard tasks only)

You aim to design a PCB schematic using SKiDL (Python) for a given circuit described in the text. Please ensure your designed circuit works properly, satisfies the requirements, and follows specific library conventions.

An example is shown below, please read it carefully.

Question

Design an isolated voltage sensing front-end using a resistor divider with an isolated amplifier to measure a high-voltage bus and output an isolated differential low-voltage sense signal.

Input node name: VIN.

Output node name: OUTP, OUTN.

Answer

Step 1

Components Needed

- **Isolated Amplifier:** AMC1350 (Precision, Isolated Amplifier).
- **Resistors:** High-voltage divider string (R1, R2, R3) to step down 400V to optimal input range (~250mV for AMC1350 linear range). R_shunt (R4) for sensing. Power
- **Supply:** High-side: VDD1 (generated from high-side floating supply). Low-side: VDD2 (3.3V system supply).
- **Decoupling Capacitors:** 100nF on both VDD1 and VDD2.
- **Input Signal Source:** VIN (High Voltage Bus).
- **Output Signals:** OUTP, OUTN (Differential output to MCU).

Design Logic

1. **Divider Network:** The 400V input needs to be scaled down. We use a string of resistors (e.g., 3x 100k) and a bottom shunt resistor to form a divider.
2. **AMC1350 Connections:**
 1. **INP/INN:** Connect across the bottom shunt resistor.
 2. **VDD1/GND1:** High-side floating power. Needs decoupling.
 3. **VDD2/GND2:** Low-side system power. Needs decoupling.
 4. **OUTP/OUTN:** Differential output.
3. **Safety:** High voltage ground (GND1) and Low voltage ground (GND2) must be separate.

Assistant Prompt (For Non-hard tasks only) Continued

Step 2

```
...python
from skidl import *

# 1. Define Nets
vin  = Net("VIN")
outp = Net("OUTP")
outn = Net("OUTN")

vdd1 = Net("VDD1") # High-side floating supply
gnd1 = Net("GND1") # High-side ground
vdd2 = Net("VDD2") # Low-side supply
gnd2 = Net("GND2") # Low-side ground

# 2. Instantiate Components
# Use "KiCAD" library for all parts.
# Footprints must follow "KiCAD:FootprintName" format.

# AMC1350: 8-pin Isolated Amplifier
# Pin 1: VDD1, 2: VINP, 3: VINN, 4: GND1
# Pin 5: GND2, 6: VOUTN, 7: VOUTP, 8: VDD2
u1 = Part("KiCAD", "AMC1350", footprint="KiCAD:SOIC-8")

# Resistor Divider (3x 100k + 1x 200R for ~250mV scaling from 400V)
# Using 0805 for standard spacing (1206 not available in lib)
r1 = Part("KiCAD", "R", value="100k", footprint="KiCAD:R_0805")
r2 = Part("KiCAD", "R", value="100k", footprint="KiCAD:R_0805")
r3 = Part("KiCAD", "R", value="100k", footprint="KiCAD:R_0805")
r_sense = Part("KiCAD", "R", value="200R", footprint="KiCAD:R_0805")

# Decoupling Capacitors (0805)
c1 = Part("KiCAD", "C", value="100nF", footprint="KiCAD:C_0805") # For VDD1
c2 = Part("KiCAD", "C", value="100nF", footprint="KiCAD:C_0805") # For VDD2

# 3. Connections

# High Voltage Divider Path
# VIN -> R1 -> R2 -> R3 -> R_sense -> GND1
vin += r1[1]
r1[2] += r2[1]
r2[2] += r3[1]
r3[2] += r_sense[1]
r_sense[2] += gnd1

# AMC1350 Low Side (Pins 5-8)
u1[5] += gnd2
u1[6] += outn
u1[7] += outp
```

User Prompt

You aim to design a PCB schematic using SKiDL (Python) for a given circuit described in the text.

Please ensure your designed circuit works properly, satisfies the requirements, and follows specific library conventions.

Assistant Prompt (For Non-hard tasks only)

You aim to design a PCB schematic using SKiDL (Python) for a given circuit described in the text. Please ensure your designed circuit works properly, satisfies the requirements, and follows specific library conventions.

An example is shown below, please read it carefully.

Question

Design an isolated voltage sensing front-end using a resistor divider with an isolated amplifier to measure a high-voltage bus and output an isolated differential low-voltage sense signal.

Input node name: VIN.

Output node name: OUTP, OUTN.

Answer**Step 1****Components Needed**

- **Isolated Amplifier:** AMC1350 (Precision, Isolated Amplifier).
- **Resistors:** High-voltage divider string (R1, R2, R3) to step down 400V to optimal input range (~250mV for AMC1350 linear range). R_shunt (R4) for sensing. Power
- **Supply:** High-side: VDD1 (generated from high-side floating supply). Low-side: VDD2 (3.3V system supply).
- **Decoupling Capacitors:** 100nF on both VDD1 and VDD2.
- **Input Signal Source:** VIN (High Voltage Bus).
- **Output Signals:** OUTP, OUTN (Differential output to MCU).

Design Logic

1. **Divider Network:** The 400V input needs to be scaled down. We use a string of resistors (e.g., 3x 100k) and a bottom shunt resistor to form a divider.

2. **AMC1350 Connections:**

1. **INP/INN:** Connect across the bottom shunt resistor.
2. **VDD1/GND1:** High-side floating power. Needs decoupling.
3. **VDD2/GND2:** Low-side system power. Needs decoupling.
4. **OUTP/OUTN:** Differential output.

3. **Safety:** High voltage ground (GND1) and Low voltage ground (GND2) must be separate.

A.3. Complete Prompts for Hard Level Tasks

User Prompt

You aim to design a PCB schematic using SKiDL (Python) for a given circuit described in the text.

Please ensure your designed circuit works properly, satisfies the requirements, and follows specific library conventions.

Assistant Prompt (For Non-hard tasks only)

You aim to design a PCB schematic using SKiDL (Python) for a given circuit described in the text. Please ensure your designed circuit works properly, satisfies the requirements, and follows specific library conventions.

An example is shown below, please read it carefully.

Question

Design an isolated voltage sensing front-end using a resistor divider with an isolated amplifier to measure a high-voltage bus and output an isolated differential low-voltage sense signal.

Input node name: VIN.

Output node name: OUTP, OUTN.

Answer

Step 1

Components Needed

- **Isolated Amplifier:** AMC1350 (Precision, Isolated Amplifier).
- **Resistors:** High-voltage divider string (R1, R2, R3) to step down 400V to optimal input range (~250mV for AMC1350 linear range). R_shunt (R4) for sensing. Power
- **Supply:** High-side: VDD1 (generated from high-side floating supply). Low-side: VDD2 (3.3V system supply).
- **Decoupling Capacitors:** 100nF on both VDD1 and VDD2.
- **Input Signal Source:** VIN (High Voltage Bus).
- **Output Signals:** OUTP, OUTN (Differential output to MCU).

Design Logic

1. **Divider Network:** The 400V input needs to be scaled down. We use a string of resistors (e.g., 3x 100k) and a bottom shunt resistor to form a divider.
2. **AMC1350 Connections:**
 1. **INP/INN:** Connect across the bottom shunt resistor.
 2. **VDD1/GND1:** High-side floating power. Needs decoupling.
 3. **VDD2/GND2:** Low-side system power. Needs decoupling.
 4. **OUTP/OUTN:** Differential output.
3. **Safety:** High voltage ground (GND1) and Low voltage ground (GND2) must be separate.

User Prompt

You aim to design a PCB schematic using SKiDL (Python) for a given circuit described in the text.

Please ensure your designed circuit works properly, satisfies the requirements, and follows specific library conventions.

Assistant Prompt (For Non-hard tasks only)

You aim to design a PCB schematic using SKiDL (Python) for a given circuit described in the text. Please ensure your designed circuit works properly, satisfies the requirements, and follows specific library conventions.

An example is shown below, please read it carefully.

Question

Design an isolated voltage sensing front-end using a resistor divider with an isolated amplifier to measure a high-voltage bus and output an isolated differential low-voltage sense signal.

Input node name: VIN.

Output node name: OUTP, OUTN.

Answer**Step 1****Components Needed**

- **Isolated Amplifier:** AMC1350 (Precision, Isolated Amplifier).
- **Resistors:** High-voltage divider string (R1, R2, R3) to step down 400V to optimal input range (~250mV for AMC1350 linear range). R_shunt (R4) for sensing. Power
- **Supply:** High-side: VDD1 (generated from high-side floating supply). Low-side: VDD2 (3.3V system supply).
- **Decoupling Capacitors:** 100nF on both VDD1 and VDD2.
- **Input Signal Source:** VIN (High Voltage Bus).
- **Output Signals:** OUTP, OUTN (Differential output to MCU).

Design Logic

1. **Divider Network:** The 400V input needs to be scaled down. We use a string of resistors (e.g., 3x 100k) and a bottom shunt resistor to form a divider.
2. **AMC1350 Connections:**
 1. **INP/INN:** Connect across the bottom shunt resistor.
 2. **VDD1/GND1:** High-side floating power. Needs decoupling.
 3. **VDD2/GND2:** Low-side system power. Needs decoupling.
 4. **OUTP/OUTN:** Differential output.
3. **Safety:** High voltage ground (GND1) and Low voltage ground (GND2) must be separate.

User Prompt

You aim to design a PCB schematic using SKiDL (Python) for a given circuit described in the text.

Please ensure your designed circuit works properly, satisfies the requirements, and follows specific library conventions.

Assistant Prompt (For Non-hard tasks only)

You aim to design a PCB schematic using SKiDL (Python) for a given circuit described in the text. Please ensure your designed circuit works properly, satisfies the requirements, and follows specific library conventions.

An example is shown below, please read it carefully.

Question

Design an isolated voltage sensing front-end using a resistor divider with an isolated amplifier to measure a high-voltage bus and output an isolated differential low-voltage sense signal.

Input node name: VIN.

Output node name: OUTP, OUTN.

Answer**Step 1****Components Needed**

- **Isolated Amplifier:** AMC1350 (Precision, Isolated Amplifier).
- **Resistors:** High-voltage divider string (R1, R2, R3) to step down 400V to optimal input range (~250mV for AMC1350 linear range). R_shunt (R4) for sensing. Power
- **Supply:** High-side: VDD1 (generated from high-side floating supply). Low-side: VDD2 (3.3V system supply).
- **Decoupling Capacitors:** 100nF on both VDD1 and VDD2.
- **Input Signal Source:** VIN (High Voltage Bus).
- **Output Signals:** OUTP, OUTN (Differential output to MCU).

Design Logic

1. **Divider Network:** The 400V input needs to be scaled down. We use a string of resistors (e.g., 3x 100k) and a bottom shunt resistor to form a divider.
2. **AMC1350 Connections:**
 1. **INP/INN:** Connect across the bottom shunt resistor.
 2. **VDD1/GND1:** High-side floating power. Needs decoupling.
 3. **VDD2/GND2:** Low-side system power. Needs decoupling.
 4. **OUTP/OUTN:** Differential output.
3. **Safety:** High voltage ground (GND1) and Low voltage ground (GND2) must be separate.

User Prompt

You aim to design a PCB schematic using SKiDL (Python) for a given circuit described in the text.

Please ensure your designed circuit works properly, satisfies the requirements, and follows specific library conventions.

Assistant Prompt (For Non-hard tasks only)

You aim to design a PCB schematic using SKiDL (Python) for a given circuit described in the text. Please ensure your designed circuit works properly, satisfies the requirements, and follows specific library conventions.

An example is shown below, please read it carefully.

Question

Design an isolated voltage sensing front-end using a resistor divider with an isolated amplifier to measure a high-voltage bus and output an isolated differential low-voltage sense signal.

Input node name: VIN.

Output node name: OUTP, OUTN.

Answer**Step 1****Components Needed**

- **Isolated Amplifier:** AMC1350 (Precision, Isolated Amplifier).
- **Resistors:** High-voltage divider string (R1, R2, R3) to step down 400V to optimal input range (~250mV for AMC1350 linear range). R_shunt (R4) for sensing. Power
- **Supply:** High-side: VDD1 (generated from high-side floating supply). Low-side: VDD2 (3.3V system supply).
- **Decoupling Capacitors:** 100nF on both VDD1 and VDD2.
- **Input Signal Source:** VIN (High Voltage Bus).
- **Output Signals:** OUTP, OUTN (Differential output to MCU).

Design Logic

1. **Divider Network:** The 400V input needs to be scaled down. We use a string of resistors (e.g., 3x 100k) and a bottom shunt resistor to form a divider.
2. **AMC1350 Connections:**
 1. **INP/INN:** Connect across the bottom shunt resistor.
 2. **VDD1/GND1:** High-side floating power. Needs decoupling.
 3. **VDD2/GND2:** Low-side system power. Needs decoupling.
 4. **OUTP/OUTN:** Differential output.
3. **Safety:** High voltage ground (GND1) and Low voltage ground (GND2) must be separate.

In the basic prompts, we utilize placeholders for the design task, input/output specifications, and component information, which are dynamically populated based on the specific requirements of each task. The component information is provided via JSON files that detail component specifications, pin definitions, and functional descriptions. Comprehensive details of

these JSON structures are available in the supplemental materials and our code repository.

For complex prompts, in addition to the component-level JSON data, we explicitly incorporate a component library introduction to prevent the LLM from losing critical contextual information during generation. Furthermore, we developed various ablation experiments for the prompts, including versions without In-Context Learning (ICL) for SKiDL code, without Chain-of-Thought (CoT) reasoning. These ablation variants are also documented in the supplemental material.

A.4. Formalization of Verification Stages and Feedback Logic

To provide a comprehensive technical overview of the PCBSchemaGen verification framework, we formalize the hierarchical stages and the corresponding feedback logic as follows:

- 1. Syntax and Electrical Foundation:** The process begins with SKiDL/Python syntax verification followed by a standard Electrical Rules Check (ERC). This stage eliminates catastrophic errors such as short circuits and floating nets, which are standard in industrial PCB EDA tools.
- 2. KG-Driven Intra-Component Verification:** Leveraging the Knowledge Graph, the verifier performs pin-level logic checks within a single IC. As shown in Table 7, specific roles like `primary_vdd` are used to ensure that internal connections strictly honor the real-world IC constraints defined in the datasheet.
- 3. KG-Driven Inter-Component Verification:** This stage validates the interface logic between the targeted IC and its external peripherals. For instance, in (Task ID #17), the verifier ensures that the power stage is correctly interfaced with essential components like gate drivers and decoupling capacitors.
- 4. SI-Based Topological Alignment and Tolerance:** By employing Subgraph Isomorphism (SI), the framework compares the generated netlist against expert-defined reference patterns. As illustrated in Figure 6, this stage distinguishes between functional errors and acceptable design variations, such as the `SI verification tolerance` for redundant components.
- 5. Closed-Loop Iterative Feedback:** Each verification stage generates interpretable error logs. These logs are injected back into the LLM as corrective prompts, enabling a training-free, self-refining design paradigm that ensures the final schematic's correctness.

A.5. Example of Multi-stage Verification and Feedback Loop based on Knowledge Graph (KG) and Subgraph Isomorphism (SI)

Since PCB schematic design lacks a universal simulation-based verification tool compatible with all real-world components, we propose a multi-stage verification and feedback loop leveraging Knowledge Graph (KG) and Subgraph Isomorphism (SI) techniques. This framework ensures the structural and topological correctness of the generated designs. We utilize a medium-level task (Task ID #7) and a hard-level task (Task ID #17) to illustrate this iterative verification and feedback process. The multi-stage verifier begins by confirming the successful generation of the SKiDL code, followed by a rigorous syntax check for both SKiDL and Python.

Once the code is syntax-error-free, a SKiDL-based Electrical Rules Check (ERC) is performed to validate electrical connectivity and design rules. The ERC is specifically designed to identify critical issues such as short circuits, unconnected pins (floating nodes), and power pin conflicts (e.g., multiple drivers on a single rail). This ERC stage is a standard procedure widely employed in industrial PCB EDA software. The following step is the topology check based on Knowledge Graph (KG) and Subgraph Isomorphism (SI).

Table 7. MGJ2D121505SC Pin Configuration and KG Roles

Pin	Name	Function	KG Role
1	+VIN	Primary positive input	<code>primary_vdd</code>
2	-VIN	Primary negative input	<code>primary_gnd</code>
5	-VOUT	Secondary negative output	<code>secondary_gnd</code>
6	0V	Secondary reference	<code>secondary_gnd</code>
7	+VOUT	Secondary positive output	<code>secondary_vdd</code>

The specific KG roles for the MGJ2D121505SC isolated DC-DC converter are outlined in Table 7. Using these roles,

we construct a KG representation of the generated schematic, which captures the components and their intra-connections. We performed a systematic verification on the critical pins check, ensuring that the primary and secondary voltage and ground pins are correctly connected according to the design specifications. For (Task ID #7), since this is an isolated DC-DC converter module, we can directly establish the expected KG role conflicts from the dataset, without exploring the comprehensive datasheet of such module. We define each pin of the IC component MGJ2D121505SC as a node, then we checked if any of two nodes that shouldn't have been connected, are wrongly connected, and vice versa. For this stage, the KG based topology verification is to checking if any of the pins in the same IC are misconnected.

The next step involves a inter-component topology check to ensure the targeted IC is correctly interfaced with external passive and active components. Take (Task ID #7) as an example: the verifier performs semantic inference to confirm that both the primary and secondary sides of the isolated DC-DC converter are connected to specific functional primitives, such as decoupling capacitors, to ensure stable operation. This stage is more challenging as it requires the LLM to understand the component's working principles and typical application circuits. If any verification fails, we provide detailed error feedback to guide the LLM in the next iteration.

Additional Subgraph Isomorphism (SI) based verification ensures the generated schematic matches expected design patterns. While human experts define reference patterns, the LLM-generated designs may vary. The SI verification extracts key subgraphs and compares them against the skeleton topology. A specific SI verification tolerance is allowed for additional nodes or edges, provided the core semantic structure is preserved. For example, in Task ID #7, the verification passes if the generated schematic contains a different number of capacitors than the reference, as long as they connect the same nodes.

The node graph visualization (Figure 6) demonstrates this process for (Task ID #7). Specifically, red nodes and nets represent intra-connection errors, blue nodes and nets represent inter-connection errors, and the yellow highlighted subgraph represents the SI verification tolerance.

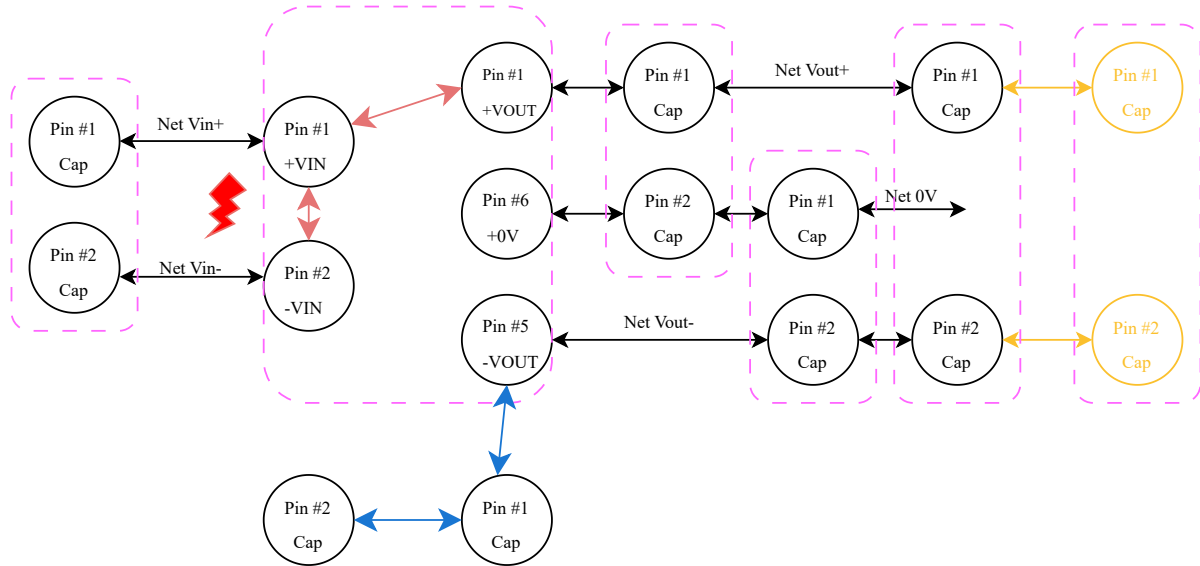


Figure 6. Multi-stage verification process for Task ID #7. Black circles denote IC pins; nodes within the purple dashed box belong to the same component. Black arrows indicate essential correct connections. Red lines mark intra-connection errors, such as the critical short circuit between +VIN and -VIN that bridges the isolation barrier, leading to hardware failure. Blue lines show inter-connection errors, e.g., a capacitor with a floating terminal. Yellow elements highlight acceptable SI-based variants, such as using two capacitors instead of one while maintaining the core topology.

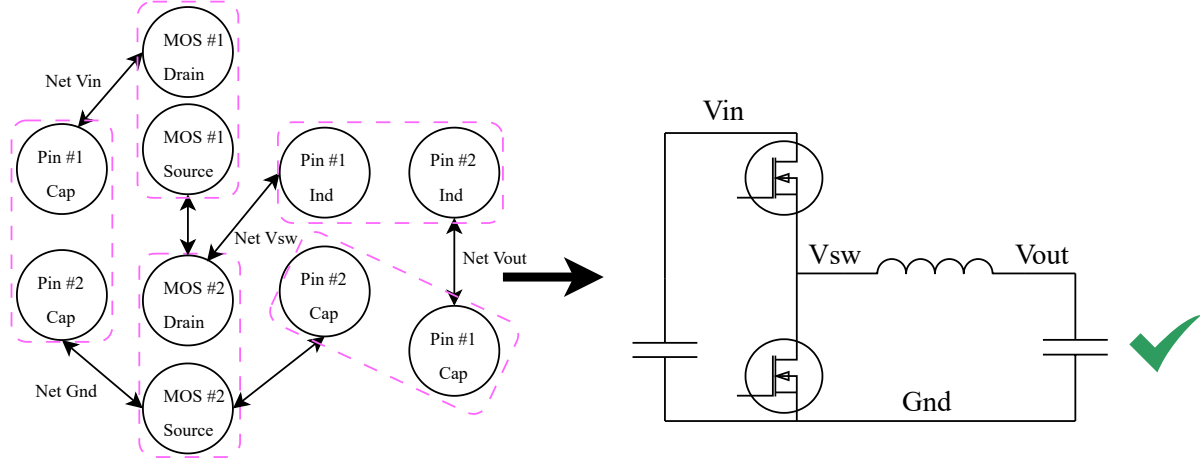


Figure 7. Visualization of hard-level Task ID #17 and its corresponding additional topology verification check. The left part illustrates the correct nodes and net connections for a synchronous buck converter, including V_{in} , V_{sw} , V_{out} , and Gnd . This core topological structure must remain consistent across all LLM-generated designs.

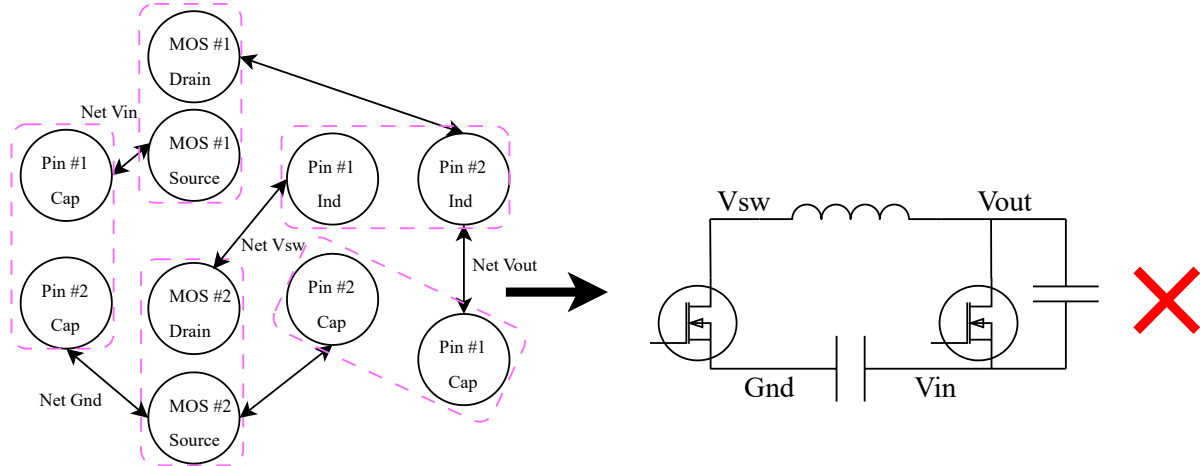


Figure 8. Visualization of an LLM-generated main power stage for Task ID #17. Although the core components are identical to the reference design, the incorrect net connections result in a dysfunctional circuit. Consequently, this design fails the topology verification check.

For hard-level tasks like (Task ID #17), the process becomes more intricate due to design complexity. We introduce an additional level of **skeleton-level semantic verification** for power electronics switch-mode power supplies. Taking the synchronous buck converter in (Task ID #17) as an example, the verifier focuses on the **major skeleton** of the power stage topology. While auxiliary components like gate drivers may vary, the core structure—including critical nodes such as the switching node, inductor node, and I/O ports—must remain consistent. Figures 7 and 8 illustrate this topology verification and feedback loop, which ensures functional correctness across all hard-level tasks.

A.6. Pin-Role Vocabulary and KG Constraints

Pin-Role Vocabulary. The Knowledge Graph assigns semantic **pin roles** to each pin of every component. These roles enable the verifier to understand pin functions without hardcoding component-specific logic. Table 8 lists all 34 pin roles organized by functional category.

Table 8. Pin-Role Vocabulary (34 roles). Each role describes the semantic function of a pin, enabling constraint checking and topology verification.

Category	Role	Description	Example
Power Supply	supply_vdd	Positive supply rail	OPA328:V+
	supply_gnd	Ground/negative rail	OPA328:V-
	primary_vdd	Isolated primary VDD	MGJ2D:+VIN
	primary_gnd	Isolated primary GND	MGJ2D:-VIN
	secondary_vdd	Isolated secondary VDD	MGJ2D:+VOUT
	secondary_gnd	Isolated secondary GND	MGJ2D:0V
Signal I/O	sense_plus	Positive sense input	AMC1350:INP
	sense_minus	Negative sense input	AMC1350:INN
	out	Single-ended output	TLV1117:OUTPUT
	out_plus	Differential output +	AMC1350:OUTP
	out_minus	Differential output -	AMC1350:OUTN
Logic	logic_in	Digital/PWM input	UCC5390E:IN+
	logic_out	Digital status output	UCC21710:RDY
Passive	passive_terminal	Generic passive pin	R:1, C:1, L:A
	diode_anode	Diode anode	D:A
	diode_cathode	Diode cathode	D:K
Buck Regulator	buck_vin	Buck input voltage	TPS54302:VIN
	buck_gnd	Buck ground	TPS54302:GND
	buck_sw	Buck switch node	TPS54302:SW
	buck_fb	Buck feedback	TPS54302:FB
	buck_en	Buck enable	TPS54302:EN
	buck_boot	Buck bootstrap	TPS54302:BOOT
Half-Bridge	halfbridge_fb	Bootstrap supply	UCC27211:HB
	halfbridge_hs	Switch node sense	UCC27211:HS
	gate_ho	High-side gate output	UCC27211:HO
	gate_lo	Low-side gate output	UCC27211:LO
MOSFET	mosfet_gate	MOSFET gate	IMZA65R015M2H:G
	mosfet_drain	MOSFET drain	IMZA65R015M2H:D
	mosfet_source	MOSFET power source	IMZA65R015M2H:S
	mosfet_kelvin_source	Kelvin sense source	IMZA65R015M2H:KS
Transformer	xfmr_primary	Primary winding	PQ5050:PRI_1
	xfmr_secondary	Secondary winding	PQ5050:SEC_1

Role Assignment. Pin roles are assigned in `kg_component.json` based on datasheet analysis and domain expertise. For example, the MGJ2D121505SC isolated DC-DC converter has:

- Pin 1 (+VIN) → primary_vdd
- Pin 2 (-VIN) → primary_gnd
- Pin 7 (+VOUT) → secondary_vdd
- Pins 5, 6 (-VOUT, 0V) → secondary_gnd

Role-Based Verification. Pin roles enable generic constraint checking. For instance, the `supply_pair` constraint can verify that *any* component's VDD and GND pins connect to distinct nets, regardless of the specific component type.

Constraint Types. The Knowledge Graph defines four constraint types that encode electrical design rules. Table 9 lists each type with its formal semantics and example error messages.

Constraint Assignment in KG. Each component in `kg_component.json` specifies its applicable constraints. For example, the OPA328 op-amp has three constraints: (1) `supply_pair` (V+, V-), (2) `differential_pair_must_be_distinct` (+IN, -IN), and (3) `must_be_connected` (+IN, -IN, OUT). This ensures that V+ and V- are not shorted, differential inputs are on different nets, and all signal pins have connections.

The domain-specific knowledge graph was constructed through a systematic methodology combining automated extraction, semantic normalization, and rigorous expert validation. The construction process consists of the following two stages.

Table 9. KG Constraint Types. Each constraint is checked during Phase 2 (fast-fail) verification. σ denotes the circuit state (net assignments).

Constraint Type	Formal Semantics	Example Error Message
supply_pair	$\text{Net}(p_{vdd}) \neq \text{Net}(p_{gnd})$ <i>VDD and GND pins must connect to distinct nets (not shorted).</i>	U1: supply pair shorted (+VIN and -VIN on VIN)
must_be_connected	$\forall p \in P : \text{Net}(p) \neq \emptyset$ <i>All specified pins must have net assignments (not floating).</i>	U1: pin FB is unconnected
driving_pair	$ \text{Endpoints}(\text{Net}(p_{gate})) \geq 2$ <i>Gate pin's net must have at least 2 endpoints (driven by something).</i>	Q1: gate net appears floating (G on GATE_H)
differential_pair_must_be_distinct	$\text{Net}(p_+) \neq \text{Net}(p_-)$ <i>Differential input pins must connect to distinct nets.</i>	U1: differential pins on same net (+IN=SENSE)

Data Sources and Extraction. For each component in our benchmark library, we aggregated open source manufacturer datasheets (e.g., Texas Instruments, Infineon, Murata) in PDF and HTML formats. We developed automated parsing scripts utilizing regular expressions and tabular data extractors to retrieve structured information. This process specifically targets Pin Configuration Tables to extract raw associations between pin numbers, names, and functional descriptions, as well as Electrical Specifications to capture quantitative operating limits, including absolute maximum ratings (voltage and current) and recommended operating conditions.

Semantic Normalization. To address terminological inconsistencies across different vendors (e.g., power pins labeled variably as V_{CC} , V_{DD} , or V_{IN}), we established a unified ontology comprising 36 distinct pin-role semantics (e.g., POWER_IN, GATE_DRIVER_OUTPUT, FEEDBACK_SENSE). We employed a hybrid mapping approach where raw pin descriptions extracted in the previous stage were projected onto this standardized ontology. This normalization layer ensures that the LLM and verifier operate on a consistent semantic plane, independent of vendor-specific naming conventions.

A.7. Error Examples Under Three Feedback Levels

Table 10. Topology Rule Error Feedback Comparison — Key Differentiation Point

Level	Feedback Message
Full	C_DIRECT missing between secondary_vdd and secondary_gnd (nets ['VISO+'] vs ['ISO_0V']) Please fix these topology issues and provide the corrected code.
Weak	Topology verification failed. Please fix these issues and provide the corrected code.
None	Attempt failed. Please try again.

Design Rationale. The three-level feedback design enables controlled ablation studies:

- **Full vs Weak:** Measures the value of pin-level error localization
- **Weak vs None:** Measures the value of knowing the error category
- **Full vs None:** Measures the total information gain from detailed feedback

As shown in Section 4 (main paper), Full feedback achieves significantly higher pass rates than Weak or None, demonstrating that pin-level error localization is critical for effective iterative refinement.

Error Type: Topology Rule Violation (C_DIRECT Missing) Scenario: The decoupling capacitor between VISO+ and ISO_0V is missing.

A.8. KiCad Component Library Construction

This section describes the custom KiCad symbol and footprint libraries developed for power electronics schematic generation. The library provides standardized component definitions that enable SKiDL-based circuit synthesis with accurate pin mappings and manufacturer-recommended land patterns. The component library is organized into three directories: symbols, footprints, and reference datasheets. This structure follows KiCad 9 conventions and enables direct integration with the SKiDL framework.

The library directory contains:

- `test.kicad_sym` – Symbol library containing 18 component symbols
- `test.pretty/` – Footprint library containing 21 land patterns (e.g., `R_0805.kicad_mod`, `C_0805.kicad_mod`, `IMZA65R015M2H.kicad_mod`)
- `datasheets/` – Reference PDF documentation (14 datasheets)

The symbol library contains 18 component definitions spanning passive elements, voltage regulators, gate drivers, power semiconductors, and magnetic components. Table 11 summarizes each symbol with its pin count and source.

Table 11. Symbol Library Contents (18 symbols). Pin counts reflect the electrical interface; mechanical pins (e.g., thermal pads) are included where applicable.

Symbol	Description	Pin Count	Source
R	Generic resistor	2	Standard
C	Generic capacitor	2	Standard
L	Generic inductor	2	Standard
D	Schottky diode (BAT165)	2	Standard
C_film	Film capacitor	2	Standard
Inductor_power	Power inductor (12-pin)	12	Custom
TLV1117-33	3.3V LDO regulator	4	TI
TPS54302	Synchronous buck regulator	8	TI
OPA328	Operational amplifier	5	TI
AMC1350	Isolated amplifier	8	TI
ACS37010	Hall-effect current sensor	6	Allegro
UCC27211	Half-bridge gate driver	14	TI
UCC27511	Low-side gate driver	6	TI
UCC21710	Isolated gate driver	16	TI
UCC5390E	Isolated gate driver	8	TI
MGJ2D121505SC	Isolated DC-DC converter	7	Murata
IMZA65R015M2H	SiC MOSFET (TOLL package)	4	Infineon
BSC052N08NS5	Si MOSFET (TDSON-8 package)	8	Infineon
transformer_PQ5050	PQ50/50 transformer	12	Custom

SKiDL provides functions for generating design artifacts compatible with KiCad 9 and downstream tools. The primary outputs include netlists, schematic visualizations, and PCB layout files.

Components are instantiated using SKiDL's `Part` constructor with library name, symbol name, and footprint specification. Pin connections use pin numbers for robustness across component variants. For example:

- Passive: `r1 = Part("test", "R", value="10k", footprint="test:R_0805")`
- Active: `ldo = Part("test", "TLV1117-33", footprint="test:TLV1117-33")`
- Pin connections: `ldo[1] += vcc (pin 1 = VIN), ldo[2] += gnd (pin 2 = GND)`

The `generate_netlist` function produces a KiCad 9 compatible netlist file for import into PCB layout tools. The `generate_svg` function creates a vector graphic representation of the schematic for documentation purposes. The `generate_pcb` function initializes a PCB file with component placements derived from the netlist, using footprints from the specified library paths.

A.9. Detailed Baseline Comparison

To comprehensively evaluate the efficacy and uniqueness of our PCBSchemaGen framework, this section provides a detailed comparison with two representative state-of-the-art baselines: CircuitLM (Hasan et al., 2026) (LLM-based) and GNN-Optimization (Plettenberg et al., 2025) (Graph Neural Network-based).

Given the fundamental differences in task scope (from module synthesis to component optimization) and output formats, a direct quantitative comparison across all dimensions is infeasible. Therefore, we present a qualitative analysis of system capabilities followed by a discussion of specific limitations. Table 12 systematically compares the frameworks across core tasks, output executability, scale, and error correction mechanisms. Our framework is the only solution capable of end-to-end system generation with executable code output and closed-loop verification.

Table 12. Qualitative comparison of capabilities. Our framework uniquely supports system-level scale and closed-loop correction.

Dimension	Ours (Full)	CircuitLM (Hasan et al., 2026)	GNN (Plettenberg et al., 2025)
Core Task	End-to-End System Gen. (Text to Netlist)	End-to-End System Gen. (Text to Netlist)	Component Optimization (Link Prediction)
Output	Executable Code (SKiDL) (Production-Ready)	Executable Code (Visualization Only)	Adjacency Matrix (Auxiliary Suggestion)
Scale	System (>100 pins) (IoT, Robot Control)	Module (~50 pins) (Sensor Breakout)	Toy (<50 nodes) (Single Filter)
Correction	Closed-Loop (Type + Location)	LLM as verifier Severe Hallucination	None (One-shot Inference)
Constraints	Hard & Soft Constraints (Real Pin/Pkg Semantics)	JSON Descriptions (Hallucination Prone)	Connectivity Only (No Pin Semantics)

1. CircuitLM (Multi-Agent LLM Generation) CircuitLM represents the state-of-the-art in using generic LLMs for circuit design, employing RAG and multi-agent collaboration to generate CircuitJSON schematics.

- **Intermediate Format vs. Engineering Code:** CircuitLM generates CircuitJSON, a format primarily designed for web-based visualization rather than industrial EDA interaction. In contrast, our **SKiDL (Python)** output is executable, compilable into standard netlists, and seamlessly integrates with PCB layout workflows.
- **Lack of Physical Verification:** Despite using a Reviewer Agent, the system relies on "open-loop" self-correction via Chain-of-Thought. Without an external datasheet-based ground truth verifier, it remains prone to hallucinations regarding pin definitions (e.g., misconnecting power pins to signal lines) and cannot reliably eliminate hard errors through iterative refinement.

2. GNN-Optimization (Graph Neural Networks) The GNN baseline (Plettenberg et al., 2025) utilizes supervised learning to predict optimizing components (e.g., decoupling capacitors) in existing graphs.

- **Task Scope Restriction:** This method performs **link prediction** rather than generation. It relies on a pre-existing partial schematic and cannot synthesize designs *tabula rasa* (from scratch).
- **Scalability Constraints:** The GNN model exhibits severe performance degradation on graphs exceeding 50 nodes, rendering it ineffective for modern PCB systems with hundreds of pins and nets.
- **Lack of Semantic Awareness:** By treating pins as undifferentiated nodes, the GNN lacks explicit modeling of "pin roles" and electrical properties, making it unsuitable for complex designs requiring strict Electrical Rule Checking (ERC).

PCBSchemaGen addresses these shortcomings through: (1) **Knowledge-Graph-Driven Verification**, which provides immutable physical constraints to eliminate hallucinations; (2) **Subgraph Isomorphism**, ensuring rigorous topological compliance beyond mere visual similarity; and (3) **Executability**, treating circuit design as software engineering to enable modular reuse and automated testing.

A.10. Sample Size and Confidence Interval

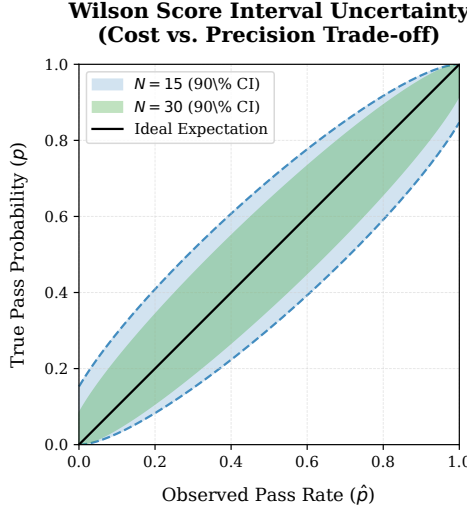
To rigorously quantify the reliability of our Pass@k metrics and balance computational efficiency with statistical validity, we utilize the **Wilson Score Interval** for binomial proportions. This method is preferred over the normal approximation (Wald interval) for small sample sizes ($n < 30$) and probabilities close to 0 or 1, as it prevents physical impossibilities (e.g., negative probabilities) and provides better coverage probability.

For an observed success rate $\hat{p} = k/n$, the confidence interval (CI) for the true success probability p at a confidence level of $1 - \alpha$ (set to 90% in our experiments, corresponding to $z \approx 1.645$) is calculated as:

$$CI = \frac{\hat{p} + \frac{z^2}{2n}}{1 + \frac{z^2}{n}} \pm \frac{z}{1 + \frac{z^2}{n}} \sqrt{\frac{\hat{p}(1 - \hat{p})}{n} + \frac{z^2}{4n^2}} \quad (4)$$

Diminishing Returns of Larger Samples. As illustrated (see generated plot), the width of the confidence interval scales approximately with $1/\sqrt{n}$. Doubling the sample size from $n = 15$ to $n = 30$ reduces the margin of error by a factor of only $1/\sqrt{2} \approx 0.707$. For example, at $\hat{p} = 0.5$, the margin of error decreases from ± 0.21 ($n = 15$) to ± 0.15 ($n = 30$).

Significance of Results. Given that our framework outperforms baselines by substantial margins (often $> 30\%$ absolute improvement in Pass@1), the confidence intervals derived from $n = 15$ are sufficiently narrow to establish statistical significance. Specifically, the lower bound of our method’s CI consistently exceeds the upper bound of the baselines’ CI, indicating that the performance gap is statistically robust and not an artifact of sampling noise. Thus, $n = 15$ represents the optimal trade-off between token cost and evaluation rigor.



A.11. Human Expert Evaluation

To validate the reliability of our multi-stage verification pipeline, we conducted a comprehensive blind study comparing automated verifier judgments against independent expert assessments.

Evaluation Methodology. We employed stratified sampling on the 23 benchmark tasks. From a total pool, we selected 460 samples (20 per task) with a strictly balanced distribution: 10 samples marked as `PASS` and 10 as `FAIL` by the verifier for each task. Three domain experts independently reviewed the generated SKiDL code and datasheets, blinded to the verifier’s decisions.

Statistical Framework. We treat human expert judgment as ground truth. Agreement is measured using Precision, Recall, F1 Score, and Cohen’s Kappa (κ). Given the balanced sampling ($N_{pass} = N_{fail}$), the expected agreement by chance is

$P_e \approx 0.5$. The metrics are defined as:

$$\text{Precision} = \frac{\text{TP}}{\text{TP} + \text{FP}}, \quad \text{Recall} = \frac{\text{TP}}{\text{TP} + \text{FN}} \quad (5)$$

$$\text{F1 Score} = 2 \cdot \frac{\text{Precision} \cdot \text{Recall}}{\text{Precision} + \text{Recall}} \quad (6)$$

$$\kappa = \frac{P_o - P_e}{1 - P_e} \approx 2P_o - 1 \quad (7)$$

Confusion Matrix Results. The detailed confusion matrices for each difficulty level (Easy, Medium, Hard) and the overall aggregation are presented below.

Table 13. Detailed Human Expert Evaluation Results. We present the confusion matrices broken down by difficulty level (a-c) and the aggregated overall performance (d), followed by the summary statistics (e).

(a) Easy Tasks ($N = 120, \kappa = 0.950$)

	Expert: P	Expert: F	Total
Ver: P	59 (TP)	1 (FP)	60
Ver: F	2 (FN)	58 (TN)	60
Total	61	59	120

(c) Hard Tasks ($N = 140, \kappa = 0.914$)

	Expert: P	Expert: F	Total
Ver: P	67 (TP)	3 (FP)	70
Ver: F	3 (FN)	67 (TN)	70
Total	70	70	140

(b) Medium Tasks ($N = 200, \kappa = 0.890$)

	Expert: P	Expert: F	Total
Ver: P	95 (TP)	5 (FP)	100
Ver: F	6 (FN)	94 (TN)	100
Total	101	99	200

(d) Overall ($N = 460, \kappa = 0.913$)

	Expert: P	Expert: F	Total
Ver: P	221 (TP)	9 (FP)	230
Ver: F	11 (FN)	219 (TN)	230
Total	232	228	460

(e) Summary of Human Expert Evaluation Metrics

Difficulty	N	κ	Precision	Recall	F1 Score
Easy	120	0.950	98.3%	96.7%	97.5%
Medium	200	0.890	95.0%	94.1%	94.5%
Hard	140	0.914	95.7%	95.7%	95.7%
Overall	460	0.913	96.1%	95.3%	95.7%

Conclusion. As summarized in Table 13e, the verifier demonstrates high consistency with human experts across all difficulty levels.

- **Strong Agreement:** $\kappa > 0.89$ across all splits, indicating robust reliability.
- **High Precision/Recall:** The system maintains $> 95\%$ precision and recall even on Hard tasks, validating the use of the automated verifier as a scalable proxy for evaluation.

A.12. Ablation Study: Subcircuit Retrieval

To investigate whether structural priors from existing designs can facilitate the generation of complex topologies, we implemented a Subcircuit Retrieval pipeline.

Experimental Design. We hypothesized that retrieving semantically similar subcircuits could serve as effective few-shot demonstrations. Our pipeline embeds task specifications using a sentence transformer and retrieves the top- k ($k = 3$) tasks based on cosine similarity. The ground truth SKiDL implementations of these retrieved subcircuits are injected into the prompt context. We evaluated this approach on the *Hard* subset (P17–P23), which features complex multi-switch architectures where pattern transfer is theoretically most beneficial. Evaluation was performed using Gemini 2.5 Flash with $n = 15$ trials per task.

Results and Negative Transfer. Table 14 presents the comparative results. Contrary to the initial hypothesis, the subcircuit retrieval approach exhibited a performance degradation ($\Delta = -9.5\%$ in overall Pass@1). While performance remained stable for standard topologies like the Synchronous Buck (P17) and LLC Primary (P21), significant regressions were observed in the Full Bridge (P18, -13.3%) and 3-Phase Motor Driver (P23, -26.6%).

Root Cause Analysis. The failure of subcircuit retrieval in this domain stems from the misalignment between *semantic similarity* in the embedding space and *topological isomorphism* in the circuit space. Tasks sharing linguistic descriptions (e.g., "isolated converter") often possess fundamentally distinct switching networks (e.g., Dual Active Bridge vs. LLC). The injection of topologically dissonant subcircuits induces **negative transfer**, causing the model to hallucinate connections based on structurally irrelevant priors rather than adhering to the target specification. This suggests that effective retrieval for circuit synthesis requires topology-aware metrics rather than purely semantic embeddings.

Table 14. Retrieval ablation results on Hard tasks (P17–P23). We compare the Non-Retrieval Baseline against the Subcircuit Retrieval approach. Pass@1 scores are derived from $n = 15$ trials. The retrieval mechanism introduces negative transfer on topologically distinct tasks, degrading overall accuracy.

Task ID	Topology Description	Non-Retrieval Pass@1 (%)	Subcircuit Retrieval Pass@1 (%)	Δ
17	Synchronous Buck	100.0	100.0	–
18	Full Bridge	80.0	66.7	-13.3
19	DAB Primary	100.0	93.3	-6.7
20	DAB Secondary	86.7	73.3	-13.4
21	LLC Primary	93.3	93.3	–
22	LLC Secondary	100.0	93.3	-6.7
23	3-Phase Motor Driver	93.3	66.7	-26.6
Overall Average		93.3	83.8	-9.5

A.13. Ablation Study: Prompt Engineering

To decouple the contributions of Chain-of-Thought (CoT) reasoning and In-Context Learning (ICL) demonstrations, we conducted a component-wise ablation study on the prompt structure.

Experimental Design. We evaluated three configurations:

- **Full Prompt (Baseline):** Includes both CoT reasoning steps and few-shot ICL examples.
- **No ICL (Zero-Shot):** Removes the few-shot examples to test the model's intrinsic knowledge of the SKiDL library, retaining only the reasoning instructions.
- **No CoT (Direct Generation):** Removes the requirement for intermediate reasoning, forcing the model to output the raw SKiDL code directly based on the ICL examples.

Quantitative Results. Table 15 summarizes the performance impact. The removal of reasoning steps (**No CoT**) resulted in the most significant degradation, dropping the Overall Pass@1 from 88.1% to 76.8% ($\Delta = -11.3\%$). In contrast, removing examples (**No ICL**) caused a more moderate decline to 82.6% ($\Delta = -5.5\%$). This hierarchy suggests that for circuit synthesis, the model's ability to plan connections is more critical than its access to syntactic references.

Role of CoT. The significant regression in the *No CoT* setting highlights the necessity of explicit reasoning. For instance, on Task P12, removing CoT caused the Pass@1 score to drop precipitously from 93.3% to 6.7%. Without CoT, the model attempts to map natural language requirements directly to netlist connections, often leading to severe connectivity errors, particularly when handling components with complex pin constraints.

Role of ICL. The *No ICL* setting primarily impacts adherence to domain-specific syntax. While the model possesses general parametric knowledge of Python, the SKiDL library requires specific instantiation patterns. The absence of few-shot demonstrations increases the frequency of API misuse and minor syntax errors, even though the underlying logical topology often remains sound.

A.14. Ablation Study: Feedback Message

To validate the effectiveness of our verification loop, we ablated the feedback strength across three levels: *Full* (providing both violation type and specific location), *Weak* (providing violation type only, with no error message or location), and *None*

Table 15. Ablation results of Prompt Engineering Skills based on Gemini 3 Flash. We compare the full prompt with variants removing in-context learning (No ICL) and chain-of-thought reasoning (No CoT). Pass@1 and Pass@5 are computed from $n = 15$ trials per task using $\widehat{\text{Pass}@k} = 1 - \binom{n-c}{k} / \binom{n}{k}$, where c is the number of successful trials.

Task ID	Gemini-3-Flash (Full)		Gemini-3-Flash (No ICL)		Gemini-3-Flash (No CoT)	
	Pass@1	Pass@5	Pass@1	Pass@5	Pass@1	Pass@5
1	100.0	100.0	100.0	100.0	100.0	100.0
2	100.0	100.0	100.0	100.0	100.0	100.0
3	73.3	100.0	73.3	100.0	20.0	73.6
4	100.0	100.0	100.0	100.0	100.0	100.0
5	100.0	100.0	100.0	100.0	100.0	100.0
6	86.7	100.0	100.0	100.0	100.0	100.0
7	100.0	100.0	100.0	100.0	100.0	100.0
8	100.0	100.0	100.0	100.0	100.0	100.0
9	100.0	100.0	100.0	100.0	100.0	100.0
10	100.0	100.0	100.0	100.0	100.0	100.0
11	100.0	100.0	100.0	100.0	100.0	100.0
12	93.3	100.0	93.3	100.0	6.7	33.3
13	100.0	100.0	100.0	100.0	100.0	100.0
14	100.0	100.0	100.0	100.0	100.0	100.0
15	100.0	100.0	100.0	100.0	100.0	100.0
16	33.3	91.6	26.7	84.6	13.3	57.1
17	100.0	100.0	26.7	84.6	100.0	100.0
18	93.3	100.0	60.0	99.8	100.0	100.0
19	100.0	100.0	60.0	99.8	100.0	100.0
20	60.0	99.8	40.0	95.8	26.7	84.6
21	0.0	0.0	0.0	0.0	0.0	0.0
22	93.3	100.0	40.0	95.8	100.0	100.0
23	93.3	100.0	80.0	100.0	100.0	100.0
Overall Pass@1 (%)	88.1	–	82.6	–	76.8	–

Table 16. Ablation results of Error Message Feedback based on Gemini 3 Flash. We compare the Full Feedback (Baseline) with variants using Weak Feedback (only error type) and No Feedback (None). Pass@1 and Pass@5 are computed from $n = 15$ trials per task. Note that for $n = 15$, any task with ≥ 11 successful trials achieves 100% Pass@5.

Task ID	Full Feedback (Baseline)		Weak Feedback		No Feedback	
	Pass@1	Pass@5	Pass@1	Pass@5	Pass@1	Pass@5
1	100.0	100.0	100.0	100.0	100.0	100.0
2	100.0	100.0	100.0	100.0	100.0	100.0
3	73.3	100.0	46.7	98.1	26.7	84.6
4	100.0	100.0	100.0	100.0	100.0	100.0
5	100.0	100.0	100.0	100.0	100.0	100.0
6	86.7	100.0	100.0	100.0	86.7	100.0
7	100.0	100.0	6.7	33.3	0.0	0.0
8	100.0	100.0	100.0	100.0	100.0	100.0
9	100.0	100.0	53.3	99.3	73.3	100.0
10	100.0	100.0	53.3	99.3	33.3	91.6
11	100.0	100.0	66.7	100.0	73.3	100.0
12	93.3	100.0	0.0	0.0	0.0	0.0
13	100.0	100.0	100.0	100.0	100.0	100.0
14	100.0	100.0	100.0	100.0	100.0	100.0
15	100.0	100.0	100.0	100.0	100.0	100.0
16	33.3	91.6	0.0	0.0	0.0	0.0
17	100.0	100.0	66.7	100.0	53.3	99.3
18	93.3	100.0	93.3	100.0	80.0	100.0
19	100.0	100.0	100.0	100.0	93.3	100.0
20	60.0	99.8	26.7	84.6	26.7	84.6
21	0.0	0.0	0.0	0.0	0.0	0.0
22	100.0	100.0	93.3	100.0	66.7	100.0
23	93.3	100.0	100.0	100.0	80.0	100.0
Overall Pass@1 (%)	88.1	–	65.5	–	64.9	–

(providing a binary pass/failed signal).

Quantitative Results. Table 4 presents the comparative performance. The data reveals that while simple tasks remain relatively insensitive to feedback granularity, **Full** feedback is indispensable for complex designs. The Overall Pass@1 dropped significantly from 88.1% in the *Full* setting to 65.5% for *Weak* and 64.9% for *None*.

Role of Explicit Localization. The performance collapse on complex tasks (e.g., P12 dropping from 93.3% to 0.0%) underscores the critical role of localization. *Full* feedback enables **precise self-correction** by explicitly pointing the model to the exact line or parameter causing the violation. In contrast, the negligible performance difference between *Weak* and *None* suggests that merely knowing the error type without localization provides insufficient context for the model to resolve structural ambiguities in the netlist, rendering it functionally equivalent to having no feedback at all.

A.15. Ablation Study: Supervised Fine-Tuning (SFT) Model

To determine if Supervised Fine-Tuning (SFT) offers a viable alternative to our feedback-driven framework, we fine-tuned GPT-4o-mini on verified (specification, code) pairs. We compared two configurations: the base model utilizing our iterative feedback framework, and a fine-tuned model using selective training data, the training data is human expert generated circuit with same components used in the task but different tasks to ensure the training integrity. This comparison tests whether internalizing domain knowledge via training is more effective than runtime verification.

As detailed in Table 17, the fine-tuned model achieves a pass rate of 44.1% (152/345), which is statistically equivalent to the base feedback model's 43.8% (151/345). While SFT shows specific gains in tasks like P1 and P13, it fails to generalize to the hardest tasks (P16–P23), showing similar limitations to the base model.

Although SFT matches the performance of our feedback framework, it introduces a critical dependency on verified training data. This limitation manifests in the "cold-start" problem, where new component libraries lack pre-existing data, and in prohibitive data acquisition costs requiring expert validation. In contrast, our feedback framework operates zero-shot without training data, offering equivalent performance with superior flexibility for practical deployment.

Table 17. Performance comparison: Base Model vs. Fine-Tuned Model.

Task	Base + Feedback	Fine-Tuned (SFT)
P1	0/15 (0%)	15/15 (100%)
P2	15/15 (100%)	15/15 (100%)
P3	7/15 (46.7%)	8/15 (53.3%)
P4	0/15 (0%)	3/15 (20.0%)
P5	15/15 (100%)	15/15 (100%)
P6	0/15 (0%)	0/15 (0%)
P7	0/15 (0%)	8/15 (53.3%)
P8	12/15 (80.0%)	15/15 (100%)
P9	1/15 (6.7%)	13/15 (86.7%)
P10	0/15 (0%)	7/15 (46.7%)
P11	2/15 (13.3%)	11/15 (73.3%)
P12	1/15 (6.7%)	11/15 (73.3%)
P13	0/15 (0%)	13/15 (86.7%)
P14	0/15 (0%)	2/15 (13.3%)
P15	2/15 (13.3%)	15/15 (100%)
P16–P18	0/15 (0%)	0/15 (0%)
P19	0/15 (0%)	1/15 (6.7%)
P20–P22	0/15 (0%)	0/15 (0%)
P23	0/15 (0%)	1/15 (6.7%)
Total Average	151/345 (43.8%)	152/345 (44.1%)

A.16. Failure Reason Analysis

To identify systematic weaknesses in model reasoning, we analyzed failure modes across difficulty levels. Errors were categorized into four types corresponding to our verification pipeline: **Phase 1** (Syntax/ERC), **Phase 2** (Knowledge Graph Constraints), **Phase 3** (Subgraph Isomorphism), and **Phase 4** (System Topology, specific to multi-switch architectures).

Table 18 and Figure 9 detail the error distribution. Three key trends emerge from the analysis:

- **Phase 1 errors decrease with difficulty** (38% on Easy vs. 9% on Hard). This counterintuitive pattern results from the richer structural templates provided in Hard task prompts, which effectively minimize syntactic ambiguity and basic pin connection errors.
- **Phase 2 errors are persistent**, dominating Easy (38%) and Medium (36%) categories. Frequent violations such as floating supply pins or omitted bootstrap capacitors validate the necessity of semantic constraints as a fast-fail filter before expensive topology matching.
- **Phase 4 errors are exclusive to Hard tasks** (33%), encompassing high-level architectural failures like malformed half-bridge structures or incorrect transformer windings. This indicates that while few-shot prompting solves syntactic issues, complex power converter synthesis requires stronger topological priors or specialized training to address system-level composition.

Table 18. Distribution of failure reasons by difficulty level (%). Percentages represent the fraction of total failures within each difficulty category. Phase 1 errors decrease in Hard tasks due to better prompting, while Phase 4 errors are unique to complex topologies.

Verification Phase	Easy	Medium	Hard
Phase 1 (Syntax + ERC)	38	26	9
Phase 2 (KG Constraint)	38	36	24
Phase 3 (Topology Check)	24	38	34
Phase 4 (System Topology)	0	0	33
Total	100	100	100

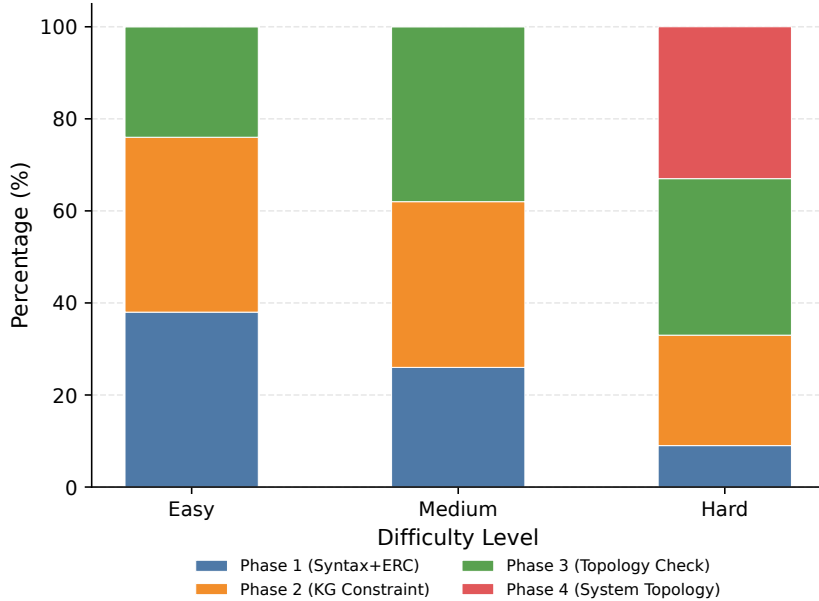


Figure 9. Stacked bar chart visualizing the distribution of failure reasons across difficulty levels. It highlights the shift from syntactic errors (Phase 1) in Easy tasks to systemic topological errors (Phase 4) exclusively in Hard tasks.